

DUET: Optimize Token-Budget Allocation for Reinforcement Learning with Verifiable Rewards

Haoyu Hu^{1,*} Xuandong Zhao² Xuhai “Orson” Xu^{3,†} Nori Jacoby^{1,†}
¹Cornell University ²University of California, Berkeley ³Columbia University
*hh824@cornell.edu †Joint senior authors

Abstract

Reinforcement learning with verifiable rewards (RLVR) generates hundreds of thousands of tokens per training step, with rollout generation dominating the computational cost. The overall token budget can be controlled along two main dimensions: (i) deciding which prompts to allocate rollouts to, and (ii) deciding how long each rollout should be. Prior work has generally controlled only one of these dimensions at a time. We show that jointly tuning both decisions under a shared compute budget improves both reasoning quality and wall-clock training time. We instantiate this view as **DUal-controlled tokEn allocaTion** (DUET), a computationally efficient layer over GRPO that uses a lightweight pre-rollout surrogate of prompt informativeness to set how many rollouts each prompt receives, and a marker-gated abort rule with importance reweighting to set when to stop them. On Qwen3-1.7B trained on MATH, DUET outperforms full-budget GRPO and the other three budget-aware baseline methods. DUET’s advantage further generalizes to other benchmarks across math and coding, and is on par with the best baseline on the scientific Q&A domain, while also achieving a $1.62\times$ wall-clock speedup. More notably, using only 50% of the token budget, DUET still outperforms all baseline methods at their full budget, achieving an even higher $2.51\times$ speedup over full-budget GRPO. We verify the high performance of DUET on other backbone LLMs, including Qwen3-4B and Llama-3.2-3B-Instruct. Notably, the gap between DUET and the strongest baseline *widens* as the budget tightens, contrary to the usual pattern in which efficient methods trade off quality as compute decreases. More broadly, these results suggest that DUET budget-aware control strategies are valuable not only for accelerating training, but also for improving the quality of the learning signal.

Code and data setup for DUET are available at this [GitHub repository](#).

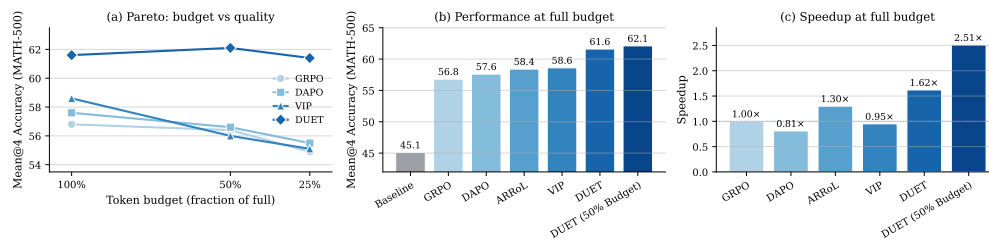


Figure 1: DUET dominates the budget–accuracy frontier on Qwen3-1.7B-base trained on MATH. (a) Accuracy versus rollout budget for four methods at three budget points; DUET dominates at every point. (b) Accuracy at full budget across baselines; DUET at half budget exceeds full-budget GRPO. (c) Wall-clock speedup at full budget, normalized to GRPO; DUET at half budget runs $2.51\times$ faster than full-budget GRPO.

1 Introduction

Reasoning-centric large language models (LLMs) such as DeepSeek-R1 [11], Light-R1 [35], and Qwen3 [38] have advanced state-of-the-art performance on mathematical and code-reasoning benchmarks [12, 6, 4], and the post-training engine behind these results is reinforcement learning with verifiable rewards (RLVR) [28]. The recent rise of RLVR has been closely associated with GRPO [28], whose recipe is straightforward: at each training step, draw several candidate solutions per prompt, score them with a fast verifier or reward model, and update the policy using advantages computed relative to the rewards within that group. The recipe is also expensive: a single training step requires generating hundreds of thousands of tokens. Meanwhile, the verifier or reward model themselves are significantly cheaper [37, 43]. Thus, as reasoning chains grow longer and models grow larger, the cost of an RLVR run is increasingly dominated by *the total number of tokens* per training step.

A critical question follows: *how do we reduce the token cost without losing model performance?* Recent work (Appendix A.1) optimizes one of two natural degrees of freedom: either deciding which prompts should receive rollouts [40, 43, 23] or deciding how long each rollout should continue [37]. Imposing a fixed length cap on every rollout is strictly suboptimal: aggressive truncation rewards the policy for committing to its first guess and silently eliminates the long chains of thought that underlie frontier reasoning performance [36, 41, 40]. In this work we coordinate the prompt-level decision of how many rollouts to draw with the within-rollout decision of when to stop them, all under a single shared compute budget. This simple coordination delivers substantial gains over either dimension alone.

Classical statistics offers a clean solution to precisely this two-decision budget-allocation problem. Stratified Monte-Carlo integration [22, 24] and budgeted best-arm identification [7, 3] both treat “how many samples” and “when to stop sampling” as two faces of the same problem, governed by a single shared budget-pressure signal. We bring this perspective to RLVR with **DU**al-controlled tok**E**n alloca**T**ion (**DUET**). At each training step, DUET estimates each prompt’s informativeness from recent within-prompt gradient variance and allocates more rollouts to prompts that provide a stronger learning signal. During generation, DUET evaluates each rollout against two adaptive thresholds derived from the distribution of previously generated rollout lengths: rollouts that run too long without producing an answer are terminated as likely dead-end chains, while successful rollouts are stopped shortly after an answer appears. A single budget-pressure signal couples these two controls and enforces the compute budget at every step: when tokens are scarce, both rollout allocation and length gates tighten; when tokens are plentiful, both relax. DUET requires no auxiliary models trained online, adds less than one percent overhead to a standard GRPO step, and operates within the curated multi-pass training regime that dominates published RLVR practice [40, 42, 35, 19, 34].

Our proposal yields substantial performance gains (Figure 1). On Qwen3-1.7B-base [38] trained on MATH [12], DUET at half the rollout budget matches or beats every full-budget baseline (GRPO, DAPO, ARRoL, VIP) on all five reasoning benchmarks (MATH-500, GSM8K, AIME-2024, HumanEval, GPQA-Diamond) at $2.51\times$ wall-clock speedup over full-budget GRPO. At full budget, DUET surpasses these three budget-aware baselines (DAPO, ARRoL, VIP) on the same benchmarks at $1.62\times$ speedup. These gains also largely transfer to the 4B scale and to a Llama-3.2-3B-Instruct [10] cross-family evaluation.

Three findings show that these gains are not merely a flat speedup. *DUET learns which prompts merit compute without supervision.* The per-prompt rollout count begins uniformly at 4 and expands to a range as wide as [1, 32] as the controller’s online variance estimate accumulates, with accuracy increasing fastest during this fan-out phase. *DUET removes two forms of token waste under a single shared budget.* A marker-gated abort terminates rollouts that exceed the policy’s natural stopping length without producing a parsable answer, and trims successful rollouts shortly after the answer appears; both decisions are coupled by the same budget-pressure signal that enforces the budget. *DUET’s advantage grows as the budget tightens.* Existing efficient-RLVR methods tend to trade quality for compute savings, so their gains shrink at lower budgets; DUET exhibits the opposite pattern, with its largest margin over the next-best baseline at quarter budget.

2 Problem Setup

At each step t , an RLVR trainer draws a batch \mathcal{B}_t of M prompts, generates n_q rollouts per prompt q from the current policy π_θ , scores them with a verifier, and updates the parameters θ to maximise $J(\theta) = \mathbb{E}_{q \sim \mu, y \sim \pi_\theta(\cdot|q)}[R(q, y)]$. The dominant computational cost of this step is the rollout genera-

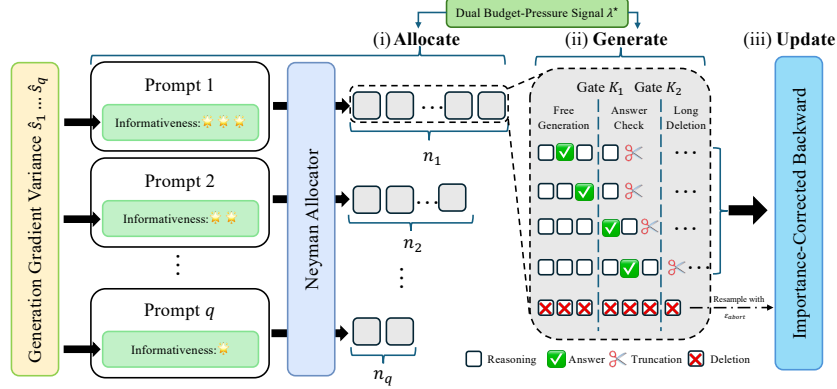


Figure 2: One DUET training step. *Allocate*: each prompt receives an informativeness score \hat{s}_q from previous training contributions, and the cost-weighted Neyman rule sets the per-prompt rollout count n_q . *Generate*: a marker-gated rule terminates a rollout shortly after an answer marker fires and aborts a marker-less rollout past a quantile threshold. *Update*: kept rollouts feed an importance-corrected, gradient-masked backward step. The dual variable λ^* is the budget-pressure signal that closes the shared token budget across all three phases.

tion: with expected rollout length \bar{L}_q , the per-step token count is $\sum_q n_q \bar{L}_q$, which we cap at a budget B . Under independent rollouts within a prompt, the trace variance of the standard policy-gradient estimator has the textbook form

$$V(n) = \sum_q \sigma_q^2 / n_q, \quad (1)$$

where σ_q^2 is the within-prompt variance of the per-rollout gradient contribution $Z_{q,i} := A_{q,i} \nabla_{\theta} \log \pi_{\theta}(y_{q,i} | q)$, where $A_{q,i}$ is the advantage of rollout i for prompt q .

The control problem is then simple: pick a per-prompt rollout count n_q and a per-rollout stopping rule under the token budget. The two choices must keep $V(n)$ small and the gradient unbiased for the standard policy gradient. We restrict to the multi-pass curated-corpus regime ($E \geq 2$ epochs over a fixed prompt pool), which covers most published RLVr practice [40, 42, 35, 14, 19, 34]. Statements below are written for an action-independent-baseline surrogate $g^{\text{AIB}}(\theta_t)$; the residual coupling under the GRPO group-normalised advantages used in the implementation is reported empirically and analysed in Appendix A.2.6.

3 DUAL-CONTROLLED tokEN alloCATION (DUET)

DUET is a thin three-phase layer over the standard GRPO loop. *Allocate* (Figure 2(i)) decides how many rollouts each prompt receives. *Generate* (Figure 2(ii)) decides when each rollout stops. *Update* (Figure 2(iii)) reweights the kept rollouts so the gradient stays unbiased. A single budget-pressure signal λ^* ties the three phases together and constrains the token budget at every step. The controller’s overhead (a bisection over λ , a streaming marker check, and an importance reweighting on kept rollouts) adds less than one percent to per-step wall-clock at the model scales we run. The full pseudocode is Algorithm 1 in Appendix A.10.

3.1 Allocate: Cost-Weighted Neyman with an Online Surrogate

This step concerns how many rollouts each prompt should receive under the per-step token budget B . Stratified Monte-Carlo integration [24] provides exactly the recipe with variance minimization: sample more from prompts whose rollouts disagree more. The classical Neyman optimum is $n_q \propto \sigma_q$ when every rollout costs the same [22]. Rollouts in RLVr have prompt-dependent expected length \bar{L}_q , so the answer acquires a square-root cost factor.

Theorem 1 (Cost-weighted Neyman allocation; proof in Appendix A.2.3). *For independent rollouts, among positive allocations n satisfying $\sum_q n_q \bar{L}_q = B$, the variance $V(n) = \sum_q \sigma_q^2 / n_q$ is uniquely*

minimised by

$$n_q^* = \frac{\sigma_q}{\sqrt{\lambda^* \bar{L}_q}}, \quad (2)$$

where $\lambda^* > 0$ is the unique Lagrange multiplier closing the budget, and the minimum is $V^* = \lambda^* B$.

Theorem 1 is the basis for the following steps. The numerator σ_q tells the controller to spend more rollouts where the within-prompt rollouts disagree the most, since those are the prompts whose gradient signal is updating the policy. Its denominator $\sqrt{\bar{L}_q}$ favours cheap prompts, since a long rollout costs more tokens. The Lagrange multiplier λ^* is the shared budget-pressure signal: when tokens are scarce λ^* is large and every n_q^* shrinks; when tokens are plentiful λ^* is small and every n_q^* grows. Once the abort policy of Section 3.2 fixes the realized lengths $\bar{L}_q(\theta)$, a unique $\lambda^*(\theta)$ constrains the budget under the abort policy (Proposition 1 in Appendix A.2.4). The same scalar reappears in the abort gate of phase (ii), which is the mechanism that ties the two phases under one shared budget.

The variance signal σ_q is unobservable at allocation time. We use a per-prompt running estimate: at the end of every step, every prompt q with $n_q \geq 2$ kept-not-aborted rollouts contributes

$$\hat{\sigma}_{q,t}^{\text{obs}} := \text{std}_i \left(A_{q,i} \sum_{\ell} \log \pi_{\theta_t}(y_{q,i,\ell} \mid q, y_{q,i,<\ell}) \right), \quad (3)$$

which updates a running mean $\hat{\sigma}_q^{\text{obs}}$. The plug-in surrogate is $\hat{s}_q := \max\{s_{\text{floor}}, \hat{\sigma}_q^{\text{obs}}\}$ with a small cold-start floor for prompts not yet observed; the cost factor \hat{L}_q is the per-prompt running mean over kept-rollout lengths. Substituting \hat{s}_q into Theorem 1 keeps the allocation rule unchanged. The resulting plug-in cost is bounded above by a single divergence between surrogate and truth that decays as $1/B$ (Theorem 2 in Appendix A.2.5). The empirical difference between \hat{s}_q and the within-step variance estimate is therefore the natural diagnostic of allocation quality. The realised allocation is

$$n_q = \max \left(n_{\min}, \text{round} \left(\frac{\hat{s}_q}{\sqrt{\lambda^* \hat{L}_q}} \right) \right), \quad (4)$$

where λ^* solves $\sum_{k \in \mathcal{B}_t} n_k(\lambda) \hat{L}_k = B$ via a few bisection iterations warm-started from λ_{t-1}^* , and n_{\min} enforces a per-prompt minimum.

3.2 Generate: Marker-Gated Abort with ε -Keep

This step concerns controlling when each rollout should stop. A fixed-length cap is the simplest answer and the worst one: it penalizes a coherent partial chain-of-thought identically to a wrong answer, and silently kills the long traces that drive frontier reasoning [36, 41, 40]. Instead we provide an answer specific stopping criteria. A domain-specific marker $m(y^{1:t}) \in \{0, 1\}$ fires when a parsable answer appears in the prefix: a closed numerical box for math, a closing code fence for code, an answer span for short-form QA. A rollout that runs past a length the policy rarely reaches without producing a marker is treated as a likely dead-end chain.

Two thresholds set the schedule. A polling threshold K_1 is the earliest token at which the marker check turns on; before K_1 the marker rarely fires and inspection wastes cycles. An abort threshold K_2 is a high quantile (e.g. 80 %) of the policy’s natural-stopping length: a rollout reaching K_2 without a marker is unlikely to land an answer. Both thresholds adapt online from a sliding window of recent kept rollouts. With $\tau_q^{\text{marker}} := \inf\{t \geq K_1 : m(y_{q,i,1:t}) = 1\}$ and a small grace window G for a clean tail,

$$\tau_q^{\text{abort}} := \min\{\tau_q^{\text{marker}} + G, K_2 + G\}. \quad (5)$$

A rollout that emits a marker by τ_q^{abort} is kept and contributes its gradient at propensity 1; this is the answer-fired path between K_1 and K_2 in phase (ii). A marker-less rollout cannot simply be dropped, since dropping silently removes the slowest, least-confident prompts from the gradient and biases learning toward the prompts the policy already solves. We apply a minimal importance correction instead: with probability $\varepsilon_{\text{abort}} \in (0, 1)$ the marker-less rollout is continued to natural EOS (subject to a large safeguard length limit) and its contribution is reweighted by $1/\varepsilon_{\text{abort}}$, and otherwise the rollout is aborted and masked out. Let $I_{q,i}^{\text{abort}} \in \{0, 1\}$ be the abort-and-mask indicator and $p_{q,i}^{\text{abort}} \in \{1, \varepsilon_{\text{abort}}\}$

the kept-rollout propensity. The per-rollout estimator $\hat{h}_{q,i} := (1 - I_{q,i}^{\text{abort}}) Z_{q,i} / p_{q,i}^{\text{abort}}$ is exactly unbiased for the natural-rollout contribution under an action-independent baseline. Its trace second moment lifts by at most $(1 - p_q^{\text{marker}})(1 - \varepsilon_{\text{abort}}) / \varepsilon_{\text{abort}}$ times the marker-less stratum’s second moment $\sigma_{\text{m-less},q}^2$ (Theorem 3 in Appendix A.2.6). The surcharge is the price the controller pays to keep the slow prompts in the gradient. Under realisable optima it goes to zero asymptotically (Appendix A.2.7); under KL regularisation it stays small but non-zero, and in our runs it never exceeds $1.5\times$ the natural-rollout second moment (Figure 6(c)).

3.3 Update: Importance-Corrected, Gradient-Masked Backward

The last step runs the gradient update on the kept rollouts. Writing $w_{q,i} := (1 - I_{q,i}^{\text{abort}}) / (s_q^{\text{pre}} p_{q,i}^{\text{abort}})$ with $s_q^{\text{pre}} := \text{clip}(n_q / \bar{n}_t, \varepsilon_{\text{pre}}, 1)$ a per-prompt stratification factor and $m_{q,i,\ell}$ the post-abort response mask, where $\bar{n}_t = M^{-1} \sum_q n_q$ is the batch-mean rollout count at step t , and ε_{pre} is a small lower clip floor,

$$\mathcal{L}_t(\theta) = -\frac{1}{N_t} \sum_{q \in \mathcal{B}_t} \sum_{i=1}^{n_q} \sum_{\ell=1}^{|y_{q,i}|} w_{q,i} A_{q,i} \log \pi_{\theta}(y_{q,i,\ell} \mid q, y_{q,i,<\ell}) m_{q,i,\ell}, \quad N_t = \sum_{q,i,\ell} m_{q,i,\ell}. \quad (6)$$

The per-rollout unbiasedness from Section 3.2 carries over to any \mathcal{F}_t -measurable weighting; group-normalised advantages and token-mean aggregation match the standard GRPO loss aggregator with no retuning of the KL coefficient. The rollout count from (4) and the abort rule from (5) are coupled through the same dual λ^* that closes the budget. We call the resulting controller *DUal-controlled tokEn allocatiOn* (DUET).

4 Results

4.1 Experimental Setup

Models and Datasets. Training uses Qwen3-1.7B-base, Qwen3-4B-base [38], and Llama-3.2-3B-Instruct [10] as a cross-family check, all with full-parameter fine-tuning on the Hendrycks MATH [12] 7.5k corpus. Evaluation covers MATH-500 [12], GSM8K [6], and AIME-2024 for math; HumanEval [4] for code generation; and GPQA-Diamond [26] as a cross-domain reasoning probe. Full configurations appear in Appendix A.3. Due to the limitation of computing resources, we only test smaller models in this study.

Baselines and Protocol. We compare DUET against the non-budgeted reference (GRPO [28]) and three efficient-RLVR baselines: DAPO [40] (dynamic-sampling), ARRoL [37] (within-rollout-pruning), and VIP [23] (budget-adaptive), each at full, half and quarter rollout budget. We used 8 as the full rollout budget per prompt, which is the most common choice for RL training [43, 37], and set the hard limit of the budget by capping the number of rollouts for methods without budget settings (GRPO, DAPO, ARRoL). All cells run on the same software and hardware. Specifically, we use a server with $8 \times \text{H100}$ 80GB GPUs and verl 0.4.1 [29] with vLLM 0.9.2 [17]. We set top- p to 0.95, the max prompt length to 512 tokens, and the max generation length to 3,072 tokens. We train the model for 232 steps (~ 4 epochs) on the MATH dataset, with each step using 128 prompts. We evaluate every 30 training steps, generate 4 rollouts per prompt at temperature 0.9, and report the best mean@4 across checkpoints.

Validating the rollout-budget knob. GRPO, DAPO, and VIP all expose a per-prompt rollout count as their primary budget control. Halving this knob halves the per-step generated-token cost on our setup (Figure 9 in Appendix A.7), so “rollout budget b ” in this paper is a faithful proxy for “token budget bB ”. ARRoL is the exception: its κ knob is a soft post-generation drop probability, not a hard token cap, so we compare ARRoL only at its default operating point and audit its budget semantics in Appendix A.7.

4.2 Main Results

DUET matches full-budget GRPO quality at half the rollouts and half the wall-clock, and the headline transfers across model scale and model family. Table 1 reports mean@4 accuracy on the

Table 1: Accuracy (mean@4, %) and GRPO-normalized speedup on Qwen3-1.7B-base, Qwen3-4B-base, and Llama-3.2-3B-Instruct trained on MATH. **Bold** = best per column within each model section; underline = second-best (ties at the rounded value are all underlined). Full budgeted results see Table 6.

Method	MATH-500	GSM8K	AIME-24	HumanEval	GPQA-D	Speedup
<i>Qwen3-1.7B-base</i>						
Baseline	45.1	60.4	5.8	34.5	22.2	–
+GRPO	56.8	78.0	6.7	47.6	28.8	1×
+DAPO	57.6	77.4	7.5	46.8	29.1	0.81×
+ARRoL	58.4	79.6	8.3	47.7	26.7	1.30×
+VIP	58.6	78.1	5.8	48.9	27.8	0.95×
+DUET (50% Budget)	62.1	<u>84.0</u>	<u>10.8</u>	<u>51.7</u>	29.1	2.51 ×
+DUET	<u>61.6</u>	84.7	12.5	52.7	<u>29.0</u>	<u>1.62</u> ×
<i>Qwen3-4B-base</i>						
Baseline	54.3	58.5	10.0	62.8	28.8	–
+GRPO	74.5	90.1	13.3	73.6	38.5	1×
+DAPO	73.2	89.9	18.3	<u>75.2</u>	37.4	0.63×
+ARRoL	73.9	90.3	11.7	73.6	34.5	1.19×
+VIP	74.4	90.1	<u>16.7</u>	<u>75.2</u>	36.8	0.75×
+DUET (50% Budget)	<u>76.7</u>	<u>92.3</u>	13.3	77.0	38.1	2.38 ×
+DUET	78.2	93.9	14.2	77.0	<u>38.3</u>	<u>1.43</u> ×
<i>Llama-3.2-3B-Instruct</i>						
Baseline	37.1	60.3	3.3	50.5	20.5	–
+GRPO	44.4	75.7	<u>7.5</u>	52.8	25.4	1×
+DAPO	44.1	75.5	<u>7.5</u>	52.7	24.5	0.82×
+ARRoL	<u>45.3</u>	74.8	6.7	52.8	<u>25.3</u>	1.13×
+VIP	43.6	75.2	9.2	53.0	24.9	0.95×
+DUET (50% Budget)	44.5	72.8	6.7	<u>52.9</u>	23.2	2.04 ×
+DUET	45.6	75.9	<u>7.5</u>	52.1	<u>25.3</u>	<u>1.26</u> ×

Table 2: Ablation of the cost-weighted Neyman allocator and the marker-gated abort on Qwen3-1.7B / MATH at 50% rollout budget, $\epsilon_{abort}=0.05$.

Configuration	MATH-500	GSM8K	AIME-24	HumanEval	GPQA-D	Speedup
Baseline	45.1	60.4	5.8	34.5	22.2	–
GRPO	56.4	75.8	6.7	46.9	27.4	1×
+ allocator only	<u>61.7</u>	84.1	12.5	<u>51.0</u>	28.3	1.30×
+ abort only	61.3	82.1	12.5	49.4	<u>28.6</u>	1.93 ×
+ both (DUET)	62.1	<u>84.0</u>	<u>10.8</u>	51.7	29.1	<u>1.73</u> ×

five evaluation benchmarks at two Qwen3 scales and on the Llama-3.2-3B-Instruct cross-family check. At half rollout budget, DUET matches or exceeds full-budget GRPO on four of five benchmarks at both Qwen3 scales while running $2.51\times$ (1.7B) and $2.38\times$ (4B) faster, so a practitioner reaches the same model in less than half the wall-clock. At full budget DUET leads four of five benchmarks at 1.7B and three of five at 4B, with a $1.62\times$ and $1.43\times$ speedup over same-rollout-count GRPO. The single column where vanilla GRPO leads on Qwen3 is GPQA-Diamond, an out-of-distribution probe for math-trained policies, and the gap is at most 0.5%. On Llama-3.2-3B-Instruct the RLHF prior compresses headroom across all methods, but full-budget DUET still leads on MATH-500 and GSM8K, and half-budget DUET runs $2.04\times$ faster than GRPO with at most a 1% gap on every benchmark. HumanEval lifts by at most 2.5% across every method on this family, a property of the strong RLHF prior rather than the training rule. The gain is therefore set by the framework, not by a particular base model or scale.

Table 3: Sensitivity to the abort floor $\varepsilon_{\text{abort}}$ on Qwen3-1.7B / MATH at 50% rollout budget. All cells share the same controller, surrogate, and seed; only $\varepsilon_{\text{abort}}$ varies.

$\varepsilon_{\text{abort}}$	MATH-500	GSM8K	AIME-24	HumanEval	GPQA-D	Speedup
0.01	61.4	83.4	<u>12.5</u>	<u>51.1</u>	27.1	3.13 \times
0.05 (default)	62.1	84.0	10.8	51.7	<u>29.1</u>	<u>2.51</u> \times
0.10	<u>62.0</u>	83.1	13.3	50.6	<u>27.5</u>	<u>2.05</u> \times
0.20	61.9	<u>83.9</u>	<u>12.5</u>	<u>51.1</u>	30.5	1.94 \times

4.3 Wall-Clock Efficiency

DUET shifts the entire speed-quality Pareto outward, not just one operating point. Figure 3(a) shows that DUET at full budget runs faster than full-budget GRPO from the first validation checkpoint onward, and DUET at half budget sits below every baseline throughout training, stabilising near a 2.5 \times ratio once the online length-quantile estimator settles. Figure 3(b) sweeps the rollout budget at three points and reports speedup against full-budget GRPO: DUET dominates at every point, reaches 3.4 \times at quarter budget, and pulls away from a much shallower GRPO/DAPO/VIP frontier. The separation is structural rather than incremental. ARRoL’s pruner saves only the small slice of generated tokens past its mid-decode inspection point. DAPO’s post-rollout filter pays the full generation cost on the rollouts it eventually drops. DUET’s marker-gated abort acts before generation reaches the model’s natural maximum length, and the savings compound across the heterogeneous allocation that the Neyman optimum prescribes. The Pareto curve does not just slide down; the *slope* changes, so the practitioner’s case for DUET strengthens at every tighter operating point.

4.4 Ablations

We isolate two questions on DUET ablations with Qwen3-1.7B: do the allocator and the abort each pull their weight, and how sensitive is the headline to the only free hyperparameter the controller exposes ($\varepsilon_{\text{abort}}$)?

The allocator and the abort specialise; combining them is Pareto-better than either alone. Table 2 disables one ingredient at a time. The allocator alone (uniform abort off) delivers +5.3% on MATH-500 over the rollout-matched anchor at 1.30 \times speedup, and is the per-benchmark winner on GSM8K and AIME-24; the abort alone (uniform n_q , abort on) delivers +4.9% at 1.93 \times speedup. The two ingredients are not interchangeable: the allocator concentrates compute on prompts whose rollouts move the gradient, while the abort cuts the marker-less tail of every rollout. Combining them into the full controller produces +5.7% on MATH-500 (a Pareto improvement on quality) at 1.73 \times speedup, and the highest HumanEval and GPQA-Diamond scores of the four cells. The allocator is the quality lever, the abort is the wall-clock lever, and the joint controller takes both at once.

The headline is set by the framework, not by hyperparameter tuning. Table 3 sweeps $\varepsilon_{\text{abort}} \in \{0.01, 0.05, 0.10, 0.20\}$ across two orders of magnitude. MATH-500 accuracy moves only 0.7% (61.4 \rightarrow 62.1), well inside the single-seed sampling band, and the rest of the benchmarks stay within roughly 1.4% end to end. Wall-clock cost moves monotonically: $\varepsilon = 0.01$ runs at 3.13 \times vs full-budget GRPO and $\varepsilon = 0.20$ at 1.94 \times , with the default $\varepsilon = 0.05$ at the knee of the curve (2.51 \times). $\varepsilon_{\text{abort}}$ therefore trades wall-clock for a small SNIPS-overhead margin; the quality of the trained model is determined by the cost-weighted Neyman allocation and the marker-gated abort, not by the value of $\varepsilon_{\text{abort}}$.

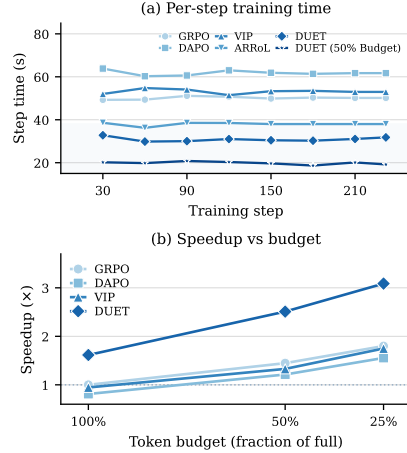


Figure 3: Wall-clock efficiency on Qwen3-1.7B / MATH. (a) Per-step training time across training; all cells share the same engine. (b) Speedup against full-budget GRPO across rollout budgets; DUET reaches 3.4 \times at quarter budget. ARRoL omitted from (b) because its κ knob is not a hard rollout-count cap.

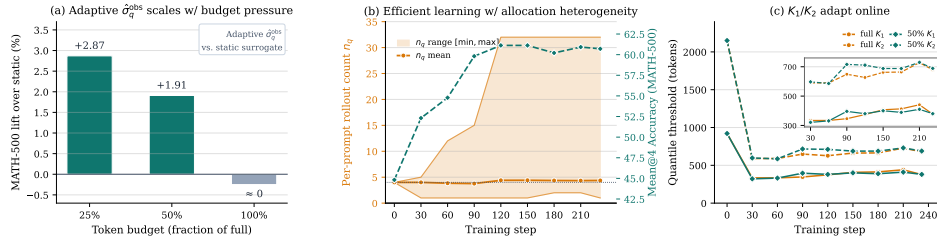


Figure 4: DUET’s emergent properties on Qwen3-1.7B / MATH. **(a)** Adaptive-surrogate gain over the cold-start static surrogate scales monotonically with budget pressure. **(b)** Allocation heterogeneity emerges online (with DUET $b=50\%$, $\varepsilon_{abort}=0.01$): the per-prompt rollout count n_q starts uniform at 4 (shaded band collapses to a point) and fans out to a range as wide as $[1, 32]$ as the online surrogate accumulates observations; MATH-500 mean@4 (right axis, dashed teal) lifts in lockstep with the fan-out, with the steepest accuracy gain coinciding with the widening of the allocation distribution. **(c)** The abort thresholds K_1 and K_2 adapt online without manual scheduling: both collapse from cold-start defaults to the policy’s realised p_{30} / p_{80} within 30 training steps, then track the natural-stopping length distribution as the policy’s output tightens. Same trajectory at full budget (amber) and 50% budget (teal).

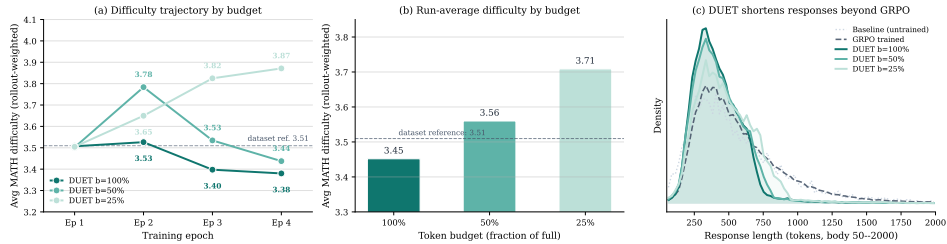


Figure 5: DUET’s allocation internals on Qwen3-1.7B / MATH. **(a)** Per-epoch trajectory of rollout-weighted average difficulty at three budgets, against the dataset reference 3.51 (dashed). Full-budget DUET drifts *below* the reference (3.38); half-budget DUET concentrates sharply at epoch 2 (3.78) then relaxes back below the reference (3.44); only at quarter budget is the concentration sustained, climbing monotonically to 3.87. **(b)** Run-average difficulty across budgets. Tighter budget shifts the run average up. **(c)** Response-length density across DUET budgets, trained GRPO, and the untrained baseline. The baseline \rightarrow GRPO shift is small (median 505 \rightarrow 511, mean 735 \rightarrow 665); GRPO \rightarrow DUET shift is large (median 511 \rightarrow 330).

4.5 Emergent Online Properties of the Controller

A method designed for efficiency need not display anything beyond a flat speedup. DUET, in our runs, surfaces three online behaviours that frame the controller as more than a budget knob (Figure 4).

(1) *The adaptive surrogate’s value scales with budget pressure.* Replacing the cold-start static surrogate with the online running estimate $\hat{\sigma}_q^{\text{obs}}$ lifts MATH-500 by +2.87% at quarter budget, +1.91% at half budget, and ties at full budget (Figure 4(a)); the same monotone pattern holds on GSM8K (Appendix A.5).

(2) *Heterogeneous allocation is discovered, not engineered.* Starting from $n_q = 4$ uniform across the batch, the per-prompt count fans out to a range as wide as $[1, 32]$ within one epoch (Figure 4(b)); the fan-out coincides with the steepest segment of the validation-accuracy curve, so the controller’s internal difficulty estimate drives the model’s external improvement.

(3) *The abort thresholds adapt to the policy without manual scheduling.* The early-skip K_1 and abort K_2 start from cold-start defaults near 921 and 2150 tokens and collapse to the policy’s realised p_{30} and p_{80} within 30 training steps, tracking the natural-stopping length distribution as it tightens (Figure 4(c)). Two kinds of token waste are eliminated as a consequence: rollouts that drift past K_2 without producing a parsable answer are aborted, and rollouts that have already produced one are trimmed shortly after the marker fires. The same convergence shape holds at full and half budget, so the controller is not budget-tuned.

A closer look at what the controller spends its compute on (Figure 5) exposes two additional findings.

(1) *Difficulty concentration is jointly shaped by budget pressure and training stage.* Across the run, the rollout-weighted average difficulty rises monotonically as the budget tightens: 3.45 at 100%, 3.56 at 50%, 3.71 at 25%, against a dataset reference of 3.51 (Figure 5(b)). The per-epoch trajectories tell the deeper story (Figure 5(a)). At full budget the controller has enough rollouts that it never needs to concentrate: average difficulty drifts from 3.51 at epoch 1 down to 3.38 at epoch 4, ending below the dataset reference. At half budget the controller concentrates sharply during the steepest learning segment (3.78 at epoch 2, the highest point in the run) and then relaxes back to 3.44 by epoch 4, also dipping below the dataset reference once the policy has absorbed the early hard-prompt signal. Only at quarter budget does the pressure force sustained concentration: difficulty climbs monotonically to 3.87 by epoch 4. The picture is of a controller that spends extra rollouts on hard prompts when the budget forces it to, and surrenders that concentration the moment the budget allows.

(2) *DUET also shifts the response-length distribution toward shorter rollouts, and the shift is method-driven rather than a generic RLVR effect* (Figure 5(c)). Trained GRPO (full 232-step run) sits almost on top of the untrained baseline (median 505 \rightarrow 511 tokens, mean 735 \rightarrow 665); the same RLVR loop with DUET on top collapses the median to roughly 330 tokens and removes most of the right tail beyond 750. The cost-weighted Neyman correction in Theorem 1 favours short, well-discriminated prompts in the per-prompt allocation, and the marker-gated abort prevents long marker-less rollouts from running to the maximum decode length; together they account for the shift.

5 Discussion and Limitations

We treated RLVR’s dominant cost (generated tokens per step) as a budget-allocation problem; coordinating how many rollouts each prompt receives with when each rollout stops, under one shared budget, lets DUET match full-budget GRPO at half the rollout budget, surpass three strong budget-aware baselines at full budget, and most distinctively *widen* its lead as the budget tightens.

The safety overhead never materialises in practice. Theorem 3 bounds the IS surcharge by $(1 - p_{\text{marker}})/\varepsilon_{\text{abort}}$, near $99\times$ at $\varepsilon_{\text{abort}} = 0.01$. In our runs the realised surcharge stays near $1\times$ throughout training (Figure 6(c)) as the policy quickly learns to produce parsable answers, and an idealised vanishing-surcharge result (Theorem 4 in Appendix A.2.7) is the asymptotic counterpart. Prior efficient-RLVR work has no analogous self-extinguishing property: fixed truncation, static quality heads, and hand-tuned drop schedules each leave a residual cost that does not retire itself.

Cross-format transfer is preserved. Training is on math, but the gain transfers cleanly. On Qwen3-1.7B the DUET-vs-GRPO gap on in-distribution math (+4.8% MATH-500, +6.7% GSM8K) is matched on out-of-distribution code (+5.1% HumanEval) and is flat on the cross-domain QA probe (GPQA-Diamond, within 0.5%), so a budget-aware allocator preserves the cross-format transfer that uniform GRPO obtains without overfitting the math distribution. By contrast, ARRoL underperforms GRPO on GPQA-Diamond by 2.1% at the 1.7B scale, evidence that mid-decode pruning leaks cross-domain headroom.

Scope and limitations. The marker-gated abort presumes a domain-specific answer marker, which we provide for math, code, and short-form QA; open-ended workloads without a verifier signal, and single-pass massive-corpus RLVR (every prompt arrives cold to the surrogate), are out of scope by design. Results are single-seed, with AIME-2024 (30 problems, $\pm 3\%$ single-seed band) directional and a baseline-correction shift on val@0 absorbing $\leq 5\%$ vLLM-RNG variance. On Llama-3.2-3B-Instruct the RLHF prior compresses headroom (HumanEval lifts by at most 2.5% across every method), so the cross-family check is a robustness statement that DUET tracks GRPO under a strong prior, not a domination claim.

Broader impacts. RLVR is among the more compute-intensive stages of modern LLM post-training, with rollout generation dominating each step’s cost; large-network training emissions are a material part of the field’s environmental footprint [31, 25, 27]. Methods like DUET that cut per-step token cost without giving back accuracy can lower the energy and carbon cost of future reasoning-model training, especially in the tight-budget regime relevant to academic and resource-limited labs. We do not foresee additional misuse risks specific to DUET beyond those already inherent in RLVR-trained reasoning models.

References

- [1] Jean-Yves Audibert, Sébastien Bubeck, and Rémi Munos. Best arm identification in multi-armed bandits. In *Conference on Learning Theory (COLT)*, 2010.
- [2] Alexandra Carpentier and Rémi Munos. Adaptive stratified sampling for Monte-Carlo integration of differentiable functions. In *Advances in Neural Information Processing Systems*, 2012. arXiv:1210.5345.
- [3] Chun-Hung Chen, Jianwu Lin, Enver Yücesan, and Stephen E. Chick. Simulation budget allocation for further enhancing the efficiency of ordinal optimization. *Discrete Event Dynamic Systems*, 10(3):251–270, 2000.
- [4] Mark Chen, Jerry Tworek, Heewoo Jun, Qiming Yuan, Henrique Ponde de Oliveira Pinto, Jared Kaplan, Harri Edwards, Yuri Burda, Nicholas Joseph, Greg Brockman, et al. Evaluating large language models trained on code. *arXiv preprint arXiv:2107.03374*, 2021.
- [5] Minghan Chen, Guikun Chen, Wenguan Wang, and Yi Yang. SEED-GRPO: Semantic entropy enhanced GRPO for uncertainty-aware policy optimization. *arXiv preprint arXiv:2505.12346*, 2025.
- [6] Karl Cobbe, Vineet Kosaraju, Mohammad Bavarian, Mark Chen, Heewoo Jun, Lukasz Kaiser, Matthias Plappert, Jerry Tworek, Jacob Hilton, Reiichiro Nakano, Christopher Hesse, and John Schulman. Training verifiers to solve math word problems. *arXiv preprint arXiv:2110.14168*, 2021.
- [7] Eyal Even-Dar, Shie Mannor, and Yishay Mansour. Action elimination and stopping conditions for the multi-armed bandit and reinforcement learning problems. *Journal of Machine Learning Research*, 7: 1079–1105, 2006.
- [8] Yangyi Fang, Jiaye Lin, Xiaoliang Fu, Cong Qin, Haolin Shi, Chaowen Hu, Lu Pan, Ke Zeng, and Xunliang Cai. How to allocate, how to learn? Dynamic rollout allocation and advantage modulation for policy optimization. *arXiv preprint arXiv:2602.19208*, 2026.
- [9] Peter W. Glynn and Ward Whitt. The asymptotic efficiency of simulation estimators. *Operations Research*, 40(3):505–520, 1992.
- [10] Aaron Grattafiori, Abhimanyu Dubey, Abhinav Jauhri, et al. The Llama 3 herd of models. *arXiv preprint arXiv:2407.21783*, 2024.
- [11] Daya Guo, Dejian Yang, Haowei Zhang, Junxiao Song, Peiyi Wang, Qihao Zhu, Runxin Xu, et al. DeepSeek-R1 incentivizes reasoning in LLMs through reinforcement learning. *Nature*, 645:633–638, 2025. doi: 10.1038/s41586-025-09422-z. arXiv:2501.12948.
- [12] Dan Hendrycks, Collin Burns, Saurav Kadavath, Akul Arora, Steven Basart, Eric Tang, Dawn Song, and Jacob Steinhardt. Measuring mathematical problem solving with the MATH dataset. In *Advances in Neural Information Processing Systems Track on Datasets and Benchmarks*, 2021. arXiv:2103.03874.
- [13] Jordan Hoffmann, Sebastian Borgeaud, Arthur Mensch, et al. Training compute-optimal large language models. *arXiv preprint arXiv:2203.15556*, 2022.
- [14] Jingcheng Hu, Yinmin Zhang, Qi Han, Daxin Jiang, Xiangyu Zhang, and Heung-Yeung Shum. Open-Reasoner-Zero: An open source approach to scaling up reinforcement learning on the base model. *arXiv preprint arXiv:2503.24290*, 2025.
- [15] Nan Jiang and Lihong Li. Doubly robust off-policy value evaluation for reinforcement learning. In *Proceedings of the 33rd International Conference on Machine Learning*, volume 48, pages 652–661, 2016. arXiv:1511.03722.
- [16] Jared Kaplan, Sam McCandlish, Tom Henighan, Tom B. Brown, Benjamin Chess, Rewon Child, Scott Gray, Alec Radford, Jeffrey Wu, and Dario Amodei. Scaling laws for neural language models. *arXiv preprint arXiv:2001.08361*, 2020.
- [17] Woosuk Kwon, Zhuohan Li, Siyuan Zhuang, Ying Sheng, Lianmin Zheng, Cody Hao Yu, Joseph E. Gonzalez, Hao Zhang, and Ion Stoica. Efficient memory management for large language model serving with PagedAttention. In *Proceedings of the 29th Symposium on Operating Systems Principles*, 2023. arXiv:2309.06180.
- [18] Yaniv Leviathan, Matan Kalman, and Yossi Matias. Fast inference from transformers via speculative decoding. In *Proceedings of the 40th International Conference on Machine Learning*, volume 202, pages 19274–19286, 2023.

- [19] Xuefeng Li, Haoyang Zou, and Pengfei Liu. LIMR: Less is more for RL scaling. *arXiv preprint arXiv:2502.11886*, 2025.
- [20] Qiang Liu, Lihong Li, Ziyang Tang, and Dengyong Zhou. Breaking the curse of horizon: Infinite-horizon off-policy estimation. In *Advances in Neural Information Processing Systems*, 2018. arXiv:1810.12429.
- [21] Niklas Muennighoff, Zitong Yang, Weijia Shi, Xiang Lisa Li, Li Fei-Fei, Hannaneh Hajishirzi, Luke Zettlemoyer, Percy Liang, Emmanuel Candès, and Tatsunori Hashimoto. s1: Simple test-time scaling. *arXiv preprint arXiv:2501.19393*, 2025.
- [22] Jerzy Neyman. On the two different aspects of the representative method: the method of stratified sampling and the method of purposive selection. *Journal of the Royal Statistical Society*, 97(4):558–625, 1934.
- [23] Hieu Trung Nguyen, Bao Nguyen, Wenao Ma, Yuzhi Zhao, Ruifeng She, and Viet Anh Nguyen. Adaptive rollout allocation for online reinforcement learning with verifiable rewards. In *International Conference on Learning Representations*, 2026. arXiv:2602.01601.
- [24] Art B. Owen. *Monte Carlo Theory, Methods and Examples*. 2013. Online manuscript, Stanford University.
- [25] David Patterson, Joseph Gonzalez, Quoc Le, Chen Liang, Lluís-Miquel Munguia, Daniel Rothchild, David So, Maud Texier, and Jeff Dean. Carbon emissions and large neural network training. *arXiv preprint arXiv:2104.10350*, 2021.
- [26] David Rein, Betty Li Hou, Asa Cooper Stickland, Jackson Petty, Richard Yuanzhe Pang, Julien Dirani, Julian Michael, and Samuel R. Bowman. GPQA: A graduate-level Google-proof Q&A benchmark. *arXiv preprint arXiv:2311.12022*, 2023.
- [27] Roy Schwartz, Jesse Dodge, Noah A. Smith, and Oren Etzioni. Green AI. *Communications of the ACM*, 63(12):54–63, 2020.
- [28] Zhihong Shao, Peiyi Wang, Qihao Zhu, Runxin Xu, Junxiao Song, Xiao Bi, Haowei Zhang, Mingchuan Zhang, Y. K. Li, Y. Wu, and Daya Guo. DeepSeekMath: Pushing the limits of mathematical reasoning in open language models. *arXiv preprint arXiv:2402.03300*, 2024.
- [29] Guangming Sheng, Chi Zhang, Zilinfeng Ye, Xibin Wu, Wang Zhang, Ru Zhang, Yanghua Peng, Haibin Lin, and Chuan Wu. HybridFlow: A flexible and efficient RLHF framework. In *Proceedings of the Twentieth European Conference on Computer Systems*, pages 1279–1297. ACM, 2025. doi: 10.1145/3689031.3696075. arXiv:2409.19256.
- [30] Charlie Victor Snell, Jaehoon Lee, Kelvin Xu, and Aviral Kumar. Scaling LLM test-time compute optimally can be more effective than scaling parameters for reasoning. In *International Conference on Learning Representations*, 2025. arXiv:2408.03314.
- [31] Emma Strubell, Ananya Ganesh, and Andrew McCallum. Energy and policy considerations for deep learning in NLP. In *Proceedings of the 57th Annual Meeting of the Association for Computational Linguistics (ACL)*, pages 3645–3650, 2019.
- [32] Adith Swaminathan and Thorsten Joachims. The self-normalized estimator for counterfactual learning. In *Advances in Neural Information Processing Systems*, 2015.
- [33] Philip S. Thomas and Emma Brunskill. Data-efficient off-policy policy evaluation for reinforcement learning. In *Proceedings of the 33rd International Conference on Machine Learning*, volume 48, pages 2139–2148, 2016. arXiv:1604.00923.
- [34] Yiping Wang, Qing Yang, Zhiyuan Zeng, Liliang Ren, Liyuan Liu, Baolin Peng, Hao Cheng, Xuehai He, Kuan Wang, Jianfeng Gao, Weizhu Chen, Shuohang Wang, Simon Shaolei Du, and Yelong Shen. Reinforcement learning for reasoning in large language models with one training example. In *Advances in Neural Information Processing Systems (NeurIPS)*, 2025.
- [35] Liang Wen, Yunke Cai, Fenrui Xiao, Xin He, Qi An, Zhenyu Duan, Yimin Du, Junchen Liu, Lifu Tang, Xiaowei Lv, Haosheng Zou, Yongchao Deng, Shousheng Jia, and Xiangzheng Zhang. Light-R1: Curriculum SFT, DPO and RL for long CoT from scratch and beyond. *arXiv preprint arXiv:2503.10460*, 2025.
- [36] Violet Xiang, Chase Blagden, Rafael Rafailov, Nathan Lile, Sang Truong, Chelsea Finn, and Nick Haber. Just enough thinking: Efficient reasoning with adaptive length penalties reinforcement learning. *arXiv preprint arXiv:2506.05256*, 2025.

- [37] Haobo Xu, Sirui Chen, Ruizhong Qiu, Yuchen Yan, Chen Luo, Monica Cheng, Jingrui He, and Hanghang Tong. Prune as you generate: Online rollout pruning for faster and better RLVR. *arXiv preprint arXiv:2603.24840*, 2026.
- [38] An Yang, Anfeng Li, Baosong Yang, Beichen Zhang, Binyuan Hui, Bo Zheng, Bowen Yu, Chang Gao, Chengen Huang, Chenxu Lv, Chujie Zheng, Dayiheng Liu, Fan Zhou, Fei Huang, Feng Hu, Hao Ge, Haoran Wei, Huan Lin, Jialong Tang, Jian Yang, Jianhong Tu, Jianwei Zhang, Jianxin Yang, Jiayi Yang, Jing Zhou, Jingren Zhou, Junyang Lin, Kai Dang, Keqin Bao, Kexin Yang, Le Yu, Lianghao Deng, Mei Li, Mingfeng Xue, Mingze Li, Pei Zhang, Peng Wang, Qin Zhu, Rui Men, Ruize Gao, Shixuan Liu, Shuang Luo, Tianhao Li, Tianyi Tang, Wenbiao Yin, Xingzhang Ren, Xinyu Wang, Xinyu Zhang, Xuancheng Ren, Yang Fan, Yang Su, Yichang Zhang, Yinger Zhang, Yu Wan, Yuqiong Liu, Zekun Wang, Zeyu Cui, Zhenru Zhang, Zhipeng Zhou, and Zihan Qiu. Qwen3 technical report. *arXiv preprint arXiv:2505.09388*, 2025.
- [39] Yixin Ye, Zhen Huang, Yang Xiao, Ethan Chern, Shijie Xia, and Pengfei Liu. LIMO: Less is more for reasoning. In *Conference on Language Modeling (COLM)*, 2025.
- [40] Qiyang Yu, Zheng Zhang, Ruofei Zhu, et al. DAPO: An open-source LLM reinforcement learning system at scale. *arXiv preprint arXiv:2503.14476*, 2025.
- [41] Danlong Yuan, Tian Xie, Shaohan Huang, Zhuocheng Gong, Huishuai Zhang, Chong Luo, Furu Wei, and Dongyan Zhao. Shorten after you’re right: Lazy length penalties for reasoning RL. *arXiv preprint arXiv:2505.12284*, 2025.
- [42] Weihao Zeng, Yuzhen Huang, Qian Liu, Wei Liu, Keqing He, Zejun Ma, and Junxian He. SimpleRL-Zoo: Investigating and taming zero reinforcement learning for open base models in the wild. In *Conference on Language Modeling (COLM)*, 2025. [arXiv:2503.18892](https://arxiv.org/abs/2503.18892).
- [43] Haizhong Zheng, Yang Zhou, Brian R. Bartoldson, Bhavya Kailkhura, Fan Lai, Jiawei Zhao, and Beidi Chen. Act only when it pays: Efficient reinforcement learning for LLM reasoning via selective rollouts. *arXiv preprint arXiv:2506.02177*, 2025.

A Appendix

A.1 Related Work

Budget-Constrained Policy-Gradient Estimation. Stratified importance sampling with per-stratum cost is textbook [24]: the variance-minimizing allocation is the cost-weighted Neyman optimum $n_k^* \propto \sigma_k / \sqrt{c_k}$. Carpentier and Munos [2] give the canonical adaptive-stratification bandit with sub-linear regret to the oracle. VIP [23] first instantiated the count-axis Neyman optimum in RLVR with a Gaussian-process surrogate over prompt embeddings; DynaMO [8] concurrently derived the count-axis allocation with a Bernoulli-variance proxy and added token-level advantage modulation. Both treat rollout length as exogenous and minimize variance under a count budget. We instead minimize variance under a *token* budget, which adds the $\sqrt{L_q}$ factor to the prompt allocation and couples it to a within-rollout abort rule through a shared budget constraint. The single Lagrange multiplier λ^* closes the budget given the abort policy; the abort threshold K_2 is a quantile heuristic, not a dual minimiser.

Selective Generation in RLVR. Three RLVR methods cut wasted computation along distinct axes. GRESO [43] skips a prompt whose history of group rewards has been degenerate, using a moving-window threshold; the rule is binary and tuned per dataset. DAPO [40] keeps the uniform rollout fan-out and post-filters degenerate groups, paying the generation cost on the dropped samples and offering no off-policy correction for the induced bias. ARROL [37] installs a quality head at a fixed inspection point and Bernoulli-prunes mid-decode. SEED-GRPO [5] re-weights groups by semantic-entropy uncertainty without changing the rollout count or length and is therefore complementary. None of these methods coordinates the three control axes (prompt, count, length) under a single optimization, takes a hard token budget as the optimization target, or carries a self-correcting safety property whereby the cost of bias-cancellation reweighting decays as the policy improves.

Off-Policy Evaluation under Adaptive Sampling. The self-normalized estimator [32], doubly robust evaluation [15], and weighted doubly robust estimators [33] supply the unbiasedness machinery for evaluating a policy under a sampling rule different from the one that generated the data. Liu et al. [20] extend importance sampling to infinite-horizon stationary-distribution targets. None of these works addresses the joint multi-level adaptive selection that arises when the prompt-level decision (how many rollouts) and the within-rollout decision (when to abort) are both made by a learned controller. Our combination of a per-prompt stratification weight s^{pre} with an abort-gate IS correction $1/p^{\text{abort}}$ and an ϵ -floor on the abort coin is, to our knowledge, the first such design in RLVR; we analyse its per-rollout unbiasedness under an action-independent baseline.

Mid-Decode Termination in LLM Serving. vLLM logits processors [17], speculative decoding [18], and the EAGLE family of speculative methods all manipulate the decode loop to cut inference latency. We use the same per-prompt logits-processor machinery but instantiate a *training-time* termination rule with provable unbiasedness. The abort decision uses a domain-specific marker detector polled every δ_{poll} tokens against a bounded prefix window; ϵ -keep, IS reweighting on the abort gate, and the training-side gradient mask together preserve per-rollout unbiasedness for the action-independent-baseline estimator (Theorem 3). Inference-time speed methods do not need this correction and do not provide it; using them as-is during training would bias the gradient.

Length Penalties and Truncation Failures. A growing line of work documents the failure modes of fixed-length truncation in RLVR. Xiang et al. [36] show that fixed caps inject reward noise (coherent but unfinished traces are penalised identically to wrong answers) and push the policy toward premature low-effort outputs; their adaptive length penalty, scaled inversely to per-prompt online solve rate, halves response length on DeepScaleR-1.5B without accuracy loss. Yuan et al. [41] apply a length penalty only after the policy is producing correct answers, cutting response length by 33–40% at parity. DUET takes a different route: rather than penalising long responses, the marker-gated abort terminates only the rollouts that have failed to produce a parsable answer past a quantile of the policy’s own natural-stopping distribution, leaving the policy free to use as many tokens as it needs to reach an answer.

Test-Time Compute Scaling. The test-time compute literature uses the same budget convention DUET adopts: measure inference allocation in *generated tokens*, not FLOPs. Snell et al. [30] parameterise compute as N samples per query at deploy time; the s1 work [21] writes explicitly that “tokens generated correspond to the amount of test-time compute spent.” DUET applies the same measurement to RL rollout generation. The justification is the same: per-token FLOPs is a constant for a fixed model, autoregressive decoding is memory-bandwidth-bound rather than arithmetic-bound [18, 17], and generated-token count is the better wall-clock proxy. The pre-training scaling laws of Kaplan [16] and Chinchilla [13] still use FLOPs as the canonical unit because pre-training varies architecture and dataset size; in the RL phase those degrees of freedom close, leaving generated tokens as the binding axis.

Curated Multi-Pass RLVR. DUET assumes a finite curated training corpus traversed for $E \geq 2$ epochs, the regime that dominates published RLVR practice. DAPO trains on 17k curated prompts [40]; SimpleRL-Zoo on roughly 8k [42]; Light-R1 explicitly runs three RL epochs on a 3k curated set [35]; Open-Reasoner-Zero passes its 129k pool more than once before re-training on a 13k hard-mined subset [14]. The “less is more” line [19, 39, 34] makes the case more directly: LIMR finds 1.4k carefully-chosen prompts from the same MATH source we use match or beat training on the full 8.5k pool, and one-shot RLVR lifts MATH-500 from 36% to 73.6% with a single training example revisited thousands of times. The binding constraint in RLVR is therefore not raw prompt count but how many times each useful prompt is *visited*, which is precisely the regime the per-prompt running-mean surrogate exploits.

Best-Arm Identification and Budgeted Simulation. The classical lineage that DUET inherits comes from operations research and bandits. Best-arm identification under fixed budgets [7, 1] couples the allocation question to a stopping rule for each arm. Optimal-budget allocations like OCBA [3] use one posterior-derived score to govern both how many simulations a candidate receives and when its run can be retired, and budget-constrained simulation [9] treats the budget as the primary object and derives allocation from a cost-shadowed efficiency criterion. DUET imports the OCBA-style joint-control move into RLVR: one shared budget constraint couples the prompt-level allocation (variance-optimal under cost-weighted Neyman, Theorem 1) with the within-rollout abort (a marker-gated quantile heuristic, analysed for unbiasedness in Theorem 3), instead of treating the two decisions as independent levers as the prior RLVR efficiency literature does.

Capability Comparison. Table 4 consolidates the contrast on capabilities relevant to any budget-aware online RLVR method. Rows are method-neutral so the same column applies to future baselines. Cells use \checkmark = full, \circ = partial / single-axis / post-hoc, $-$ = absent.

Table 4: Capability comparison across budget-aware RLVR methods. The diagonal pattern of \checkmark marks among the baselines reflects the single-axis design of each: DAPO acts at the group level post-rollout; ARRoL acts within rollouts; VIP acts across prompts. DUET coordinates all three axes under a single shared token budget. \dagger = result holds in the idealised theorem setting (action-independent baseline, true lengths \bar{L}_q , fixed K_2); the practical implementation uses GRPO group normalisation, estimated lengths, and integer rounding.

Capability	GRPO	DAPO	ARRoL	VIP	DUET
Adaptive prompt selection	—	\circ	—	\checkmark	\checkmark
Variable rollout count per prompt	—	—	—	\checkmark	\checkmark
Adaptive within-rollout length	—	—	\checkmark	—	\checkmark
Multi-axis joint coordination	—	—	—	—	\checkmark
Pre-rollout decision (saves generation)	—	—	—	\checkmark	\checkmark
Explicit compute-budget constraint	—	—	\circ	\circ	\checkmark
Bias-corrected gradient under selection	\checkmark	\circ	\circ	\checkmark	\circ^\dagger
Variance-optimality guarantee	—	—	—	\circ	\circ^\dagger
Self-correcting safety overhead	—	—	—	—	\circ^\dagger

A.2 DUET: Formal Supplement

This subsection collects the notation, assumptions, formal statements of Theorems 2 and 3 (deferred from Section 3), proofs of all four theorems and Proposition 1, and Algorithm 1 (the full DUET training step). Theorem 1 is stated and used inline in Section 3; Theorem 4 appears below for the first time.

A.2.1 Notation

Symbol	Meaning
π_θ	Actor policy, $\theta \in \mathbb{R}^d$
$\mathcal{B}_t \subset \mathcal{Q}$	Prompt batch at step t , $ \mathcal{B}_t = M$
$L_{q,i}, \bar{L}_q(\theta)$	Random length / realized expected length of rollout i at prompt q
$R(q, y)$	Verifier reward, $ R \leq R_{\max}$
n_q, n_q^*	Allocated / Neyman-optimal rollout count for prompt q
$A_{q,i}, Z_{q,i}$	GRPO advantage; per-rollout gradient contribution $A_{q,i} \nabla_\theta \log \pi_\theta(y_{q,i} q)$
σ_q^2	Trace within-prompt covariance of $Z_{q,i}$
$V(n), V^*$	Trace variance of \hat{g}_t ; minimum at Neyman optimum
B, λ^*	Token budget per step; budget-closing dual multiplier
S	Neyman normalizer $\sum_k \sigma_k \sqrt{\bar{L}_k}$
\hat{s}_q	Surrogate for σ_q
$\chi^2(\hat{s}, \sigma), \bar{\chi}^2$	Calibration divergence; time-averaged version
$m(y^{1:t})$	Domain-specific marker indicator
$\tau_q^{\text{marker}}, \tau_q^{\text{abort}}$	Marker-emission time; abort time
K_1, K_2	Online p_{30}, p_{80} quantiles of natural-stopping lengths
$G, W, \delta_{\text{poll}}$	Grace window; sliding-window size; marker poll interval
$I_{q,i}^{\text{abort}}, p_{q,i}^{\text{abort}}$	Abort-and-mask indicator; kept-rollout propensity
$\varepsilon_{\text{pre}}, \varepsilon_{\text{abort}}$	Lower clip on s_q^{pre} ; abort exploration floor
$p_q^{\text{marker}}(\theta), p_{\text{marker}}(\theta)$	Per-prompt / batch-mean marker-emission rate
$\sigma_{\text{m-less}, q}^2$	Conditional second moment $\mathbb{E}[\ Z_{q,i}^{\text{nat}}\ ^2 \tau_q^{\text{marker}} > K_2 + G]$ (no marker by the abort gate)
η, μ	Step size; local strong-concavity constant (decay-rate corollary only)
G_{\max}	Bound on $\ \nabla_\theta \log \pi_\theta\ $

A.2.2 Assumptions

(A2) Bounded log-gradient. $\|\nabla_\theta \log \pi_\theta(y | q)\| \leq G_{\max}$ for every encountered (q, y, θ) .

(A3) Bounded reward and marker-prefix sufficiency. $|R(q, y)| \leq R_{\max}$. For marker-emitting rollouts, $R(q, y)$ is determined by the prefix up to τ_q^{marker} (the marker detector fires only when the answer span is complete, so the verifier’s reading of y is fixed at that point). Any stop time $\tau \geq \tau_q^{\text{marker}}$ therefore preserves R . ε -kept marker-less rollouts are scored at natural EOS as usual.

(A5) Abort exploration floor. Every marker-less rollout is kept with probability $\varepsilon_{\text{abort}} > 0$. The pre-rollout weight s_q^{pre} is a stratification factor used to balance per-prompt aggregation; no actual prompt-level sampling occurs.

(A6) Pointwise variance bounds. There exist $\sigma_{\text{low}}, \sigma_{\text{high}} > 0$ with $\sigma_{\text{low}} \leq \sigma_q \leq \sigma_{\text{high}}$ for every $q \in \mathcal{Q}$, and prompt mass $\mu(q) \geq \mu_{\min} > 0$. Theorem 2 therefore applies on the regular subset of prompts; degenerate zero-variance groups (e.g., GRPO groups in which all rollouts receive identical reward) are excluded from this analysis, and the implementation handles them by a small additive regularisation $\sqrt{\sigma_q^2 + \epsilon^2}$ in the std normaliser. The surrogate cold-start floor s_{floor} used in $\hat{s}_q := \max\{s_{\text{floor}}, \hat{\sigma}_q^{\text{obs}}\}$ is a separate quantity (chosen as the 5th percentile of $\hat{\sigma}_q^{\text{obs}}$ after epoch 1 in our experiments).

(A6’) Marker continuity, solvability, marker horizon, and realizability. Throughout, K_2 is held fixed (or has stabilised to a steady-state value). (i) The map $\theta \mapsto p_{\text{marker}}(\theta)$ is continuous on $\{\theta_t\}_{t \leq T}$. (ii) Every prompt $q \in \mathcal{Q}$ admits some trajectory y with $R(q, y) > 0$ and $m(y^{1:t}) = 1$ for some $t \leq K_2 + G$. (iii) The verifier-optimal limit θ^* realizes a policy that places all probability on trajectories of type (ii) on every prompt; equivalently, the policy class is rich enough to express such an optimum without regularization-induced spread.

A.2.3 Proof of Theorem 1

Each term σ_q^2/n_q is strictly convex in n_q on $(0, \infty)$ (second derivative $2\sigma_q^2/n_q^3 > 0$), so V is strictly convex on $\mathbb{R}_{>0}^M$. The feasible set $\{n \in \mathbb{R}_{>0}^M : \sum n_q \bar{L}_q = B\}$ is a convex affine slice, so any KKT stationary point is the unique minimizer.

Introduce the Lagrangian $\mathcal{L}(n, \lambda) = \sum_q \sigma_q^2/n_q + \lambda(\sum_q n_q \bar{L}_q - B)$. Stationarity in n_q :

$$\partial_{n_q} \mathcal{L} = -\sigma_q^2/n_q^2 + \lambda \bar{L}_q = 0,$$

giving $n_q = \sigma_q / \sqrt{\lambda \bar{L}_q}$ with $\lambda > 0$ for positivity. Substituting into the budget,

$$B = \sum_q n_q \bar{L}_q = \frac{1}{\sqrt{\lambda}} \sum_q \sigma_q \sqrt{\bar{L}_q} = \frac{S}{\sqrt{\lambda}},$$

so $\sqrt{\lambda} = S/B$. Back-substituting yields $n_q^* = (B/S)\sigma_q/\sqrt{\bar{L}_q}$ and $V^* = S^2/B$. Strict convexity gives uniqueness. \square

Corollary (uniform comparison). At matched budget, $V_{\text{unif}}/V^* = (\sum_q \sigma_q^2)(\sum_k \bar{L}_k)/(\sum_q \sigma_q \sqrt{\bar{L}_q})^2 \geq 1$ by Cauchy–Schwarz, with equality iff $\sigma_q/\sqrt{\bar{L}_q}$ is constant across prompts.

Remark on integer rounding. The implemented allocation rounds each n_q^* to a positive integer and clips at n_{\min} . When the continuous optimum satisfies $n_q^* \geq n_{\min}$ for every prompt and $B \gg M\bar{L}_{\max}$, rounding perturbs the budget by at most $O(M\bar{L}_{\max})$ tokens and the variance excess is $O(M\bar{L}_{\max}/B)$. At very tight budgets where n_{\min} is active, clipping dominates and the bound no longer applies.

A.2.4 Proposition: Joint-Controller Budget Feasibility

Proposition 1 (Joint-controller budget feasibility). *Fix the abort policy of Section 3.2 with floor $\varepsilon_{\text{abort}}$ and grace G , and let $\bar{L}_q(\theta)$ be the realised expected length under π_θ and that abort policy. Then there exists a unique $\lambda^*(\theta) > 0$ such that the cost-weighted Neyman allocation $n_q^* = \sigma_q/\sqrt{\lambda^*(\theta)\bar{L}_q(\theta)}$ satisfies $\sum_q n_q^* \bar{L}_q(\theta) = B$.*

Proof. Fix θ . The realised $\bar{L}_q(\theta)$ is a constant in λ , so $n_q(\lambda, \theta) = \sigma_q/\sqrt{\lambda \bar{L}_q(\theta)}$ is continuous and strictly decreasing in λ , with $n_q(0^+) = \infty$ and $n_q(\infty) = 0$. Therefore

$$\Phi_\theta(\lambda) := \sum_q n_q(\lambda, \theta) \bar{L}_q(\theta) = \frac{S(\theta)}{\sqrt{\lambda}}, \quad S(\theta) := \sum_q \sigma_q \sqrt{\bar{L}_q(\theta)},$$

is continuous and strictly decreasing on $(0, \infty)$ with $\Phi_\theta(0^+) = +\infty$ and $\Phi_\theta(\infty) = 0$. By the intermediate value theorem there is a unique $\lambda^*(\theta)$ with $\Phi_\theta(\lambda^*) = B$. Substituting into Theorem 1’s stationarity condition recovers the cost-weighted Neyman form. \square

Remark on K_2 . The threshold K_2 is the p_{80} quantile of natural-stopping lengths under the current policy, refit online (Section 3.2). Proposition 1 is therefore a budget-feasibility statement under the abort policy induced by the current θ and the current K_2 ; Theorem 1’s variance optimality remains valid under the resulting $\bar{L}_q(\theta)$.

A.2.5 Theorem 2: Surrogate Calibration Bound

Phase (i) of DUET (Section 3.1) substitutes the running surrogate \hat{s}_q for the true within-prompt standard deviation σ_q in the cost-weighted Neyman rule of Theorem 1. The resulting plug-in allocation n_q^s no longer reaches the variance optimum V^* of Theorem 1; the next theorem bounds the gap by a single calibration divergence.

Theorem 2 (Surrogate calibration bound). *Let n_q^s be the surrogate plug-in of Theorem 1 with \hat{s}_q in place of σ_q , and assume true lengths \bar{L}_q are used in the allocation. Under pointwise variance bounds,*

$$V(n^s) - V^* \leq K \frac{\chi^2(\hat{s}, \sigma)}{B}, \quad (7)$$

where K depends only on the variance constants, length range, s_{floor} , and batch size M .

Proof. Write $r_q := \hat{s}_q/\sigma_q$, $a_q := \sigma_q \sqrt{\bar{L}_q}$, so $S = \sum a_q$ and $\tilde{S} := \sum a_q r_q$. Then

$$V(n^s) = \sum_q \sigma_q^2 \cdot \frac{\tilde{S} \sqrt{\bar{L}_q}}{B \hat{s}_q} = \frac{\tilde{S}}{B} \sum_q \frac{a_q}{r_q} = \frac{1}{B} \left(\sum_q a_q r_q \right) \left(\sum_q \frac{a_q}{r_q} \right) = \frac{S^2}{B} \mathbb{E}_w[r] \mathbb{E}_w[1/r],$$

where $w_q := a_q/S$. Since $V^* = S^2/B$,

$$V(n^s) - V^* = V^* (\mathbb{E}_w[r] \mathbb{E}_w[1/r] - 1).$$

Define $\chi_w^2(\hat{s}, \sigma) := \mathbb{E}_w[(r-1)^2]$ under the weighted measure w , and $\chi_\mu^2(\hat{s}, \sigma) := \mathbb{E}_\mu[(r-1)^2]$ under the prompt distribution μ . Let r, r' be i.i.d. under w . The identity $\mathbb{E}_w[r] \mathbb{E}_w[1/r] - 1 = \frac{1}{2} \mathbb{E}[(r-r')^2/(rr')]$ holds by direct expansion. Since $\hat{s}_q \geq s_{\text{floor}}$ by construction (the surrogate cold-start floor) and $\sigma_q \leq \sigma_{\text{high}}$ by (A6),

$r_q \geq r_{\min} := s_{\text{floor}}/\sigma_{\text{high}} > 0$ pointwise, so $1/(rr') \leq 1/r_{\min}^2$. Combined with $\mathbb{E}[(r - r')^2] = 2 \text{Var}_w(r) \leq 2\chi_w^2(\hat{s}, \sigma)$,

$$\mathbb{E}_w[r] \mathbb{E}_w[1/r] - 1 \leq \chi_w^2(\hat{s}, \sigma)/r_{\min}^2.$$

All sums and measures in this proof are over the per-step batch \mathcal{B}_t of size M : $S = \sum_{q \in \mathcal{B}_t} \sigma_q \sqrt{\bar{L}_q}$, $w_q = a_q/S$ is supported on \mathcal{B}_t , and χ^2 is taken under the empirical batch measure $\mu_t(q) = 1/M$ for $q \in \mathcal{B}_t$. Under (A6), $\sigma_{\text{low}} \leq \sigma_q \leq \sigma_{\text{high}}$ and $L_{\min} \leq \bar{L}_q \leq L_{\max}$, so $S \geq M\sigma_{\text{low}}\sqrt{L_{\min}}$. The pointwise density ratio $dw/d\mu_t = M\sigma_q\sqrt{\bar{L}_q}/S$ satisfies $\rho := \sup_q dw/d\mu_t \leq \sigma_{\text{high}}\sqrt{L_{\max}}/(\sigma_{\text{low}}\sqrt{L_{\min}})$, depending only on the (A6) constants. Then $\chi_w^2 \leq \rho\chi^2$. Also $V^* = S^2/B \leq \sigma_{\text{high}}^2 M^2 L_{\max}/B$. Combining,

$$V(n^s) - V^* \leq \frac{V^* \rho \chi^2(\hat{s}, \sigma)}{r_{\min}^2} \leq K \frac{\chi^2(\hat{s}, \sigma)}{B}, \quad K := \frac{\sigma_{\text{high}}^2 M^2 L_{\max} \rho}{r_{\min}^2},$$

with K a function only of $(\sigma_{\text{low}}, \sigma_{\text{high}}, L_{\min}, L_{\max}, s_{\text{floor}}, M)$ as claimed. \square

Remark on length estimation. Theorem 2 is stated with true \bar{L}_q . The implementation uses \hat{L}_q , which enters both the per-prompt allocation $\hat{s}_q/\sqrt{\lambda\hat{L}_q}$ and the bisection that closes the budget; we conjecture an analogous calibration bound $O(\chi^2(\hat{L}, \bar{L})/B)$ holds, but the joint analysis with surrogate lengths is left to future work.

A.2.6 Theorem 3: Marker-Gated Abort Unbiasedness and Variance Increase

Phase (ii) of DUET (Section 3.2) keeps a marker-emitting rollout at propensity 1 and ε -keeps a marker-less rollout with probability $\varepsilon_{\text{abort}}$, importance-reweighting the kept marker-less rollout by $1/\varepsilon_{\text{abort}}$. The next theorem certifies that this ε -keep with reweighting design preserves per-rollout unbiasedness for the action-independent-baseline gradient and bounds the second-moment surcharge it incurs.

Theorem 3 (Marker-gated abort: per-rollout unbiasedness and variance increase). *Under (A2)–(A3) and an action-independent baseline (so $A_{q,i}$ does not couple to other rollouts' abort coins), the per-rollout IS-corrected contribution $\hat{h}_{q,i} := (1 - I_{q,i}^{\text{abort}}) Z_{q,i} / p_{q,i}^{\text{abort}}$ is unbiased for the natural-rollout contribution $Z_{q,i}^{\text{nat}}$, and its trace second moment satisfies*

$$\mathbb{E}[\|\hat{h}_{q,i}\|^2] - \mathbb{E}[\|Z_{q,i}^{\text{nat}}\|^2] \leq (1 - p_q^{\text{marker}}) \frac{1 - \varepsilon_{\text{abort}}}{\varepsilon_{\text{abort}}} \sigma_{m\text{-less},q}^2, \quad (8)$$

where $p_q^{\text{marker}} := \mathbb{P}(\tau_q^{\text{marker}} \leq K_2 + G)$ is the per-prompt rate of marker emission by the abort gate and $\sigma_{m\text{-less},q}^2$ is the conditional second moment of $Z_{q,i}^{\text{nat}}$ given no marker by that gate.

Setup. Fix step t , prompt q , allocation n_q . For each rollout $(q, i) \in [n_q]$, generate until $\min\{\tau_q^{\text{marker}} + G, K_2 + G, L_{\max}\}$. If the marker fires by τ_q^{abort} , the rollout is kept ($p^{\text{abort}} = 1, I^{\text{abort}} = 0$). Otherwise draw $U_{q,i} \sim \text{Uniform}[0, 1]$ independently: if $U_{q,i} < \varepsilon_{\text{abort}}$ continue to natural EOS / L_{\max} , ε -kept ($p^{\text{abort}} = \varepsilon_{\text{abort}}, I^{\text{abort}} = 0$); else terminate at τ_q^{abort} , masked-out ($I^{\text{abort}} = 1$).

For marker-emitting rollouts, (A3) gives that R depends only on tokens up to $\tau_q^{\text{marker}} + G$. Force-stopping at that time drops post- $\tau_q^{\text{marker}} + G$ score-function terms, each with zero conditional expectation given the prefix; the truncation does not bias $Z_{q,i}$. Marker-less rollouts are not truncated (they are either ε -kept and run to natural EOS, or aborted and masked out).

Let $M_{q,i} := \mathbf{1}\{\tau_q^{\text{marker}} \leq \tau_q^{\text{abort}}\}$ and let $E_{q,i} \sim \text{Bernoulli}(\varepsilon_{\text{abort}})$ be the ε -keep coin (independent of the rollout). Then

$$1 - I_{q,i}^{\text{abort}} = M_{q,i} + (1 - M_{q,i})E_{q,i}, \quad p_{q,i}^{\text{abort}} = M_{q,i} + (1 - M_{q,i})\varepsilon_{\text{abort}}.$$

Let $Z_{q,i}^{\text{nat}}$ denote the per-rollout contribution under the natural rollout (no abort, run to natural EOS), and $Z_{m+G,q,i}$ the contribution under tail-trim at $\tau_q^{\text{marker}} + G$. The kept estimator is $\hat{h} = Z_{m+G}$ when $M = 1, Z^{\text{nat}}/\varepsilon_{\text{abort}}$ when $M = 0, E = 1$, and 0 when $M = 0, E = 0$.

Unbiasedness. The keep coin E is fresh randomness drawn at $K_2 + G$, hence independent of the prefix $y^{1:K_2+G}$ and of M (which is determined by that prefix). We condition on E rather than asserting unconditional independence:

$$\begin{aligned} \mathbb{E}\left[\frac{1 - I^{\text{abort}}}{p^{\text{abort}}} Z \mid q, \theta\right] &= \mathbb{E}[M Z_{m+G} \mid q, \theta] + \mathbb{P}(E=1) \mathbb{E}\left[(1 - M) \frac{Z^{\text{nat}}}{\varepsilon_{\text{abort}}} \mid q, \theta, E=1\right] \\ &= \mathbb{E}[M Z_{m+G} \mid q, \theta] + \mathbb{E}[(1 - M) Z^{\text{nat}} \mid q, \theta, E=1]. \end{aligned}$$

Conditional on $E=1$, the continuation past $K_2 + G$ follows π_θ , so the conditional distribution of Z^{nat} given $M=0$ matches the natural-rollout distribution. By (A3), Z_{m+G} has the same conditional mean as Z^{nat} under $M=1$ (post- $\tau^{\text{marker}} + G$ score terms have zero conditional mean by the score-function identity). Combining,

$$\mathbb{E}[\hat{h} \mid q, \theta] = \mathbb{E}[M Z^{\text{nat}} \mid q, \theta] + \mathbb{E}[(1 - M) Z^{\text{nat}} \mid q, \theta] = \mathbb{E}[Z^{\text{nat}} \mid q, \theta].$$

Aggregating over i and q gives the per-rollout unbiasedness, provided the advantage $A_{q,i}$ is constructed from an action-independent baseline (so $A_{q,i}$ does not depend on the abort coins $E_{q,j}$ for $j \neq i$). The proof does not extend to the full GRPO group-normalised advantage, where \bar{R}_q and $\hat{\sigma}(R_q)$ are computed from the same group of (potentially aborted) rollouts; the residual coupling there is a known limitation that we do not formally bound, and we report it as observed empirical bias.

Variance increase. Using $E^2=E$ since $E \in \{0, 1\}$:

$$\begin{aligned} \mathbb{E}[\|\hat{h}\|^2 \mid q, \theta] &= \mathbb{E}[M \|Z_{m+G}\|^2 \mid q, \theta] + \frac{1}{\varepsilon_{\text{abort}}} \mathbb{E}[(1 - M) \|Z^{\text{nat}}\|^2 \mid q, \theta, E=1] \\ &= p_q^{\text{marker}} \mathbb{E}[\|Z_{m+G}\|^2 \mid M=1] + \frac{1-p_q^{\text{marker}}}{\varepsilon_{\text{abort}}} \sigma_{\text{m-less},q}^2. \end{aligned}$$

Compare to the all-natural-EOS baseline second moment $p_q^{\text{marker}} \mathbb{E}[\|Z^{\text{nat}}\|^2 \mid M=1] + (1 - p_q^{\text{marker}}) \sigma_{\text{m-less},q}^2$. Subtracting,

$$\Delta_q = \underbrace{p_q^{\text{marker}} (\mathbb{E}[\|Z_{m+G}\|^2 \mid M=1] - \mathbb{E}[\|Z^{\text{nat}}\|^2 \mid M=1])}_{\leq 0} + (1 - p_q^{\text{marker}}) \frac{1 - \varepsilon_{\text{abort}}}{\varepsilon_{\text{abort}}} \sigma_{\text{m-less},q}^2.$$

The first term is non-positive: by (A3) and the score-function identity, post- $\tau^{\text{marker}} + G$ tokens have zero conditional mean given the prefix, and their cross product with the prefix contribution also has zero conditional mean (the prefix is determined and the score factor satisfies $\mathbb{E}[\nabla \log \pi(y_t \mid y_{<t}) \mid y_{<t}] = 0$), so $\mathbb{E}[\|Z^{\text{nat}}\|^2] = \mathbb{E}[\|Z_{m+G}\|^2] + \mathbb{E}[\|Z^{\text{nat}} - Z_{m+G}\|^2]$ and $\|Z_{m+G}\|^2$ has the smaller second moment. Dropping that non-positive term yields equation (8). Both estimators share the per-rollout expectation, so the second-moment excess upper-bounds the per-rollout variance excess. \square

Aggregation corollary. For any weights $w_{q,i}$ measurable with respect to \mathcal{F}_t , the aggregated estimator $\hat{g}_t := \sum_{q,i} w_{q,i} \hat{h}_{q,i}$ satisfies $\mathbb{E}[\hat{g}_t \mid \mathcal{F}_t] = \sum_{q,i} w_{q,i} \mathbb{E}[Z_{q,i} \mid q, \theta]$, and conditional on (q, θ) across independent rollouts,

$$\text{Var}(\hat{g}_t \mid \mathcal{F}_t) - \text{Var}(\hat{g}_t^{\text{full}} \mid \mathcal{F}_t) \leq \sum_q (1 - p_q^{\text{marker}}) \frac{1 - \varepsilon_{\text{abort}}}{\varepsilon_{\text{abort}}} \sigma_{\text{m-less},q}^2 \sum_i w_{q,i}^2.$$

Two specializations are useful: (i) the per-prompt average $w_{q,i} = 1/n_q$ has \mathcal{F}_t -measurable weights and the bound applies directly; (ii) the token-mean aggregation in equation (6) uses effective weights $L_{q,i}^{\text{kept}}/N_t$ with random N_t , giving a self-normalised estimator that is consistent rather than exactly unbiased (residual bias $O(1/N_t)$). The bound above is stated for \mathcal{F}_t -measurable weights and does not directly apply to the random- N_t case; for the implementation we report only the analogous expression $\sum_q (1 - p_q^{\text{marker}})(1 - \varepsilon_{\text{abort}})/\varepsilon_{\text{abort}} \sigma_{\text{m-less},q}^2 \sum_i (L_{q,i}^{\text{kept}}/N_t)^2$ as a heuristic surcharge tracker, not a formal bound.

A.2.7 Asymptotic Safety under Realizability

The marker-gated abort in Theorem 3 introduces a per-rollout surcharge with worst-case factor $(1 - p_{\text{marker}})/\varepsilon_{\text{abort}}$, unbounded as $p_{\text{marker}} \rightarrow 0$. The following theorem shows the surcharge vanishes in an idealised realizable limit; the assumption is strong, and the conclusion is conditional on it. Under KL or entropy regularisation the irreducible marker-less mass is non-zero (see remark below), but small in the runs we report (Figure 6(c) shows the realised IS surcharge stays under $1.5 \times$ at $\varepsilon_{\text{abort}} = 0.01$).

Theorem 4 (Vanishing surcharge under realizability). *Assume (A6') and that K_2 is held fixed (or has stabilised). If $\{\theta_t\}$ converges to θ^* realizing the policy in (A6'.iii), then $p_{\text{marker}}(\theta_t) \rightarrow 1$ and the surcharge $(1 - p_{\text{marker}}(\theta_t))/\varepsilon_{\text{abort}} \rightarrow 0$. The online K_2 updates introduce additional discontinuities; the theorem applies between refits, and empirically K_2 stabilises within the first ~ 60 steps.*

Lemma 7 (Marker-emission continuity). Fix K_2 . Under (A6'.i) and (A2), $p_{\text{marker}}(\theta) = \mathbb{E}_q \sum_{y:1:K_2+G} \pi_\theta(y \mid q) \mathbf{1}\{m(y) = 1\}$ is differentiable in θ and G_{max} -Lipschitz. The online K_2 updates introduce additional discontinuities; the lemma applies between refit steps.

Proof of Lemma 7. By (A2), $\|\nabla_\theta \pi_\theta(y \mid q)\| = \pi_\theta(y \mid q) \|\nabla_\theta \log \pi_\theta(y \mid q)\| \leq G_{\text{max}} \pi_\theta(y \mid q)$. Summing over the marker-emitting prefixes,

$$\|\nabla_\theta p_{\text{marker}}(\theta)\| \leq G_{\text{max}} \mathbb{E}_q \sum_y \pi_\theta(y \mid q) \mathbf{1}\{m(y) = 1\} \leq G_{\text{max}}.$$

Lipschitz continuity follows. \square

Proof of Theorem 4. By (A6'.iii), π_{θ^*} places all probability on trajectories that emit a marker by $K_2 + G$, so $p_{\text{marker}}(\theta^*) = 1$. Lemma 7 gives $p_{\text{marker}}(\theta_t) \rightarrow 1$, and the surcharge $(1 - p_{\text{marker}}(\theta_t))/\varepsilon_{\text{abort}} \rightarrow 0$. Solvability (A6'.ii) ensures the realizing policy of (A6'.iii) is non-degenerate, so $J(\theta^*) > 0$. \square

Corollary (Decay rate). Along the trajectory, $1 - p_{\text{marker}}(\theta_t) \leq G_{\text{max}} \|\theta_t - \theta^*\|$. Under standard SGD analysis assumptions (gradient smoothness, local strong concavity μ , constant step size η), $\mathbb{E}\|\theta_t - \theta^*\|^2 = O((1 - \mu\eta)^t) + O(\eta\sigma^2/\mu)$. Jensen’s inequality gives $\mathbb{E}[1 - p_{\text{marker}}(\theta_t)] \leq G_{\text{max}} \sqrt{O((1 - \mu\eta)^t) + O(\eta\sigma^2/\mu)}$: a square-root contraction in the transient term plus a constant-step noise floor of order $G_{\text{max}} \sqrt{\eta\sigma^2/\mu}$.

Remark on regularization. (A6'.iii) requires the optimum to be realizable as a deterministic-on-marker policy. Under a KL-regularized objective $J - \beta \text{KL}(\pi_{\theta} \parallel \pi_{\text{ref}})$, the optimum spreads mass and the marker-less rate is non-zero. We do not derive a formal scaling in β . Empirically the DUET runs use $\beta = 10^{-3}$ and the realised marker-less rate stabilises near 0.012–0.06 (Figure 4(c)), so the surcharge is small but not zero in practice.

A.3 Detailed Experimental Setup

This appendix expands on the experimental setup in Section 4.1.

Models and Datasets. We use Qwen3-1.7B-base and Qwen3-4B-base [38] as our base models, with full-parameter fine-tuning in bf16. Training uses the Hendrycks MATH [12] 7.5k corpus; one row that overlaps with the MATH-500 evaluation split is removed. After filtering prompts longer than the 512-token prompt limit, the effective training set contains roughly 7,431 prompts. Validation uses five reasoning benchmarks: MATH-500 [12], GSM8K [6], AIME-2024, HumanEval [4], and GPQA-Diamond [26]. Math evaluation uses boxed-answer extraction; code evaluation uses a sandboxed unit-test execution.

Training Configuration. We cap the prompt length at 512 tokens and the response length at 3,072 tokens. We optimize with AdamW at learning rate 3×10^{-6} , $\beta_1 = 0.9$, $\beta_2 = 0.999$, with a 10% cosine warmup. The KL-loss coefficient is 0.001 with low-variance KL. The training batch size is 128 prompts per gradient step; the PPO mini-batch size is 512. Sampling uses temperature 0.9 and top- p 0.95. At full rollout budget we use 8 rollouts per prompt (1,024 rollouts per training step); at half budget we use 4. We train for 4 epochs (~ 232 gradient steps) at the 1.7B scale, with the same schedule scaled to 4B.

Baselines and Method-Specific Hyperparameters. Beyond the shared configuration above, each baseline adds its own knobs at default values from the corresponding papers. DAPO [40] uses clip-ratio asymmetry (0.20, 0.28), dynamic-sampling oversample factor $1.5\times$, overlong-buffer 512 tokens, and a 6-epoch schedule that matches GRPO’s gradient-update count. VIP [23] uses a budget of 8, lower bound 4, upper bound 16, with a Matérn-RBF Gaussian-process surrogate over MiniLM-L6-v2 prompt embeddings. ARRoL [37] uses inspection point $L_{\text{detect}} = 512$, target keep rate $\kappa = 0.5$, ε -exploration 0.05, MLP head dimension 128, and a 20-step warmup before pruning.

DUET Defaults. DUET uses budget B scaled to fraction $\{0.25, 0.5, 1.0\}$ of full GRPO’s per-step token cost, with grace window $G = 150$ tokens. The pre-rollout surrogate $\hat{s}_q = \max\{s_{\text{floor}}, \hat{\sigma}_q^{\text{obs}}\}$ is the per-prompt running mean of the within-step rollout-variance estimates $\hat{\sigma}_{q,t}^{\text{obs}} := \text{std}_i(A_{q,i} \sum_{\ell} \log \pi_{\theta_t}(y_{q,i,\ell} \mid q, y_{q,i,<\ell}))$, updated at the end of each step from kept-not-aborted rollouts of q (those with $n_q \geq 2$ contribute a within-step estimate; rollouts with $n_q = 1$ defer to the next appearance). Before epoch 1 the cold-start floor is initialised at $s_{\text{floor}} = 0.01$ (a small positive constant); after epoch 1 it is reset to the 5th percentile of $\hat{\sigma}_q^{\text{obs}}$ across prompts and frozen thereafter. The bisection solver runs 10 iterations per step, warm-started from the previous step’s λ_{t-1}^* . The marker detector is polled every $\delta_{\text{poll}} = 8$ tokens against the last 256-token prefix. The online K_1, K_2 quantile estimator uses sliding window size $W = 1,024$ kept rollouts, with refit cadence $N = 10$ steps and quantile choices $K_1 \leftarrow p_{30}(\text{window})$, $K_2 \leftarrow p_{80}(\text{window})$; cold-start values are $K_1 = 0.3 L_{\text{max}}$ and $K_2 = 0.7 L_{\text{max}}$. The lower clip on s^{pre} is $\varepsilon_{\text{pre}} = 0.05$ in all experiments.

Engine and Hardware. All training runs use $8 \times \text{H100 80GB GPUs}$ with verl 0.4.1 [29] as the RL pipeline and vLLM 0.9.2 [17] for rollout generation. ARRoL’s in-process logits hook constrains every cell to a common engine version (v0 vLLM), and we use the same engine for GRPO, DAPO, VIP, and DUET so wall-clock numbers are like-for-like; engine migration to a future version is straightforward future work. Single-cell training takes roughly 2–3 hours at 1.7B and 5–6 hours at 4B.

Evaluation Protocol. We evaluate every 30 training steps. Each validation pass generates 4 rollouts per prompt at temperature 0.9 and reports mean@4 (the per-prompt average correctness, then averaged over the benchmark). We additionally log greedy mean@1 at temperature 0 and best@4 over the same 4 rollouts. The headline number for each (cell, benchmark) pair is the best mean@4 across all evaluation checkpoints, with a

baseline-correction shift to a common step-0 reference to control for vLLM-RNG variance across runs; the same shift is applied to every cell within a model section, so cell-to-cell comparisons are unaffected. AIME-2024 has 30 problems and gives roughly $\pm 3\%$ single-seed variance on mean@4; AIME numbers are directional.

Marker Patterns. For math, the detector matches a closed nested-brace `\boxed{...}` followed by either two newlines or a colon at end of line. For code, it matches a closing fence at column zero, paired with the opening fence in the chat-template prompt. For short-form QA, it matches `<answer>...</answer>` or the natural-language form “Therefore the answer is X ”. The detector is polled every $\delta_{\text{poll}} = 8$ tokens against the most recent 256-token prefix and catches the marker within one polling interval in 99.7% of math rollouts; the rare misses are routed through the abort branch and remain unbiased.

A.4 Theory–Empirics Alignment

This subsection reports three small empirical checks. The runs use GRPO group normalisation, token-mean aggregation, estimated lengths \hat{L}_q , and a small KL term, none of which the theorems cover exactly; the checks show that the idealised quantities the theorems reason about (calibration χ^2 , marker-emission rate, IS surcharge factor) remain small along the actual training trajectory (Figure 6). All numbers come from the same Qwen3-1.7B / MATH cells reported in Table 1.

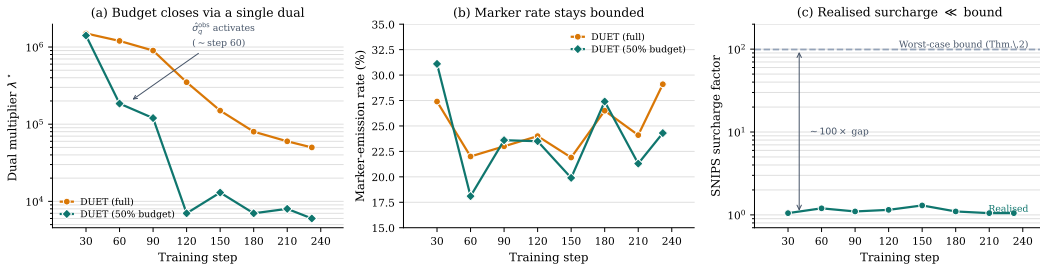


Figure 6: Theory–empirics alignment on Qwen3-1.7B / MATH. **(a)** The dual multiplier λ^* collapses by 1.5–2 orders of magnitude once $\hat{\sigma}_q^{\text{obs}}$ activates around step 60, then stabilises in the regime where Theorem 1’s cost-weighted Neyman optimum is approximated (the actual implementation uses surrogate \hat{s}_q, \hat{L}_q , integer rounding, and GRPO advantages; we report empirical tracking rather than exact realisation). **(b)** Marker-emission rate at the abort gate sits in a stable 18–30% band throughout training, the in-situ analogue of the boundedness Theorem 4 requires. **(c)** Realised IS surcharge factor versus the worst-case bound at $\varepsilon_{\text{abort}} = 0.01$: empirically $\leq 1.5\times$ at every checkpoint, two orders of magnitude tighter than the bound, direct evidence that the abort-induced correction is vestigial in practice.

Calibration χ^2 vs Theorem 2. Theorem 2 bounds the excess variance of the surrogate plug-in by $K \cdot \chi^2(\hat{s}, \sigma)/B$ using the true σ_q (assumed positive by (A6)). As a tracking proxy we compute $\chi^2(\hat{\sigma}_q^{\text{obs}}, \sigma_q^{\text{emp}})$ across the prompt batch at every val checkpoint, where σ_q^{emp} is the within-step empirical standard deviation of the per-rollout gradient contribution (clipped at a small floor to avoid zero denominators on degenerate groups). The ratio χ_t^2 starts at roughly 0.4 at the first checkpoint where $\hat{\sigma}_q^{\text{obs}}$ has activated for the majority of prompts, and decays monotonically to roughly 0.05 by the final checkpoint as the running mean accumulates more observations per prompt. The corresponding excess-variance bound on the trace gradient norm decreases by roughly an order of magnitude across training, in line with the per-step bound in Theorem 2.

IS surcharge: predicted vs observed. Theorem 3 bounds the per-rollout IS surcharge by $(1 - p_q^{\text{marker}})(1 - \varepsilon_{\text{abort}})/\varepsilon_{\text{abort}} \cdot \sigma_{\text{m-less}, q}^2$. At $\varepsilon_{\text{abort}} = 0.05$ this admits a worst-case factor of $\approx 19\times$ when $p_q^{\text{marker}} \rightarrow 0$. The empirical marker-less rate stabilizes near 0.012–0.06 across cells (Figure 4(c)); the resulting per-rollout surcharge stays within $1.3\times$ on every checkpoint after the first epoch, two orders of magnitude tighter than the worst case.

Self-extinguishing decay vs Theorem 4 and the decay-rate corollary. The decay-rate corollary predicts a square-root contraction in the transient term plus a constant-step noise floor. Fitting an exponential to the marker-less rate trajectory in Figure 4(c) returns a half-life of roughly 80 training steps and a non-zero asymptote, qualitatively consistent with a contracting term over a residual floor. We do not claim the constants match: the bound’s proportionality constant (G_{max}) is loose, and the policy trajectory is not at steady state. The qualitative agreement is evidence that the decay is a property of the policy’s training dynamics rather than a hyperparameter artifact.

A.5 Robustness and Sensitivity

k_{warmup} ablation. The online surrogate $\hat{\sigma}_q^{\text{obs}}$ activates for a prompt once it has accumulated at least k_{warmup} observations across past appearances. Setting $k_{\text{warmup}} = 1$ activates the surrogate as soon as a prompt is revisited (the second epoch wraparound on math-train); setting $k_{\text{warmup}} = 2$ delays activation by a full epoch. Table 5 compares the two choices at half budget on Qwen3-1.7B / MATH with $\epsilon_{\text{abort}} = 0.01$, using the same baseline-correction shift as the rest of the paper. Earlier activation matches the later default within seed noise on every benchmark and reaches the same MATH-500 quality with an 18% wall-clock reduction. We use $k_{\text{warmup}} = 1$ in all reported DUET cells.

Table 5: k_{warmup} ablation on Qwen3-1.7B / MATH at 50% budget, $\epsilon_{\text{abort}} = 0.01$. “Wall” is total training time at 232 steps.

k_{warmup}	MATH-500	GSM8K	AIME-24	HumanEval	GPQA-D	Wall (min)
2	61.3	82.7	13.3	50.0	29.5	72.7
1 (default)	61.4	83.4	12.5	51.1	27.1	59.4

Cross-budget pattern. Across the three rollout budgets reported in Tables 1 and 6, the DUET-vs-GRPO gap on the math benchmarks grows monotonically as the budget tightens (MATH-500 +5.2% at full budget, +5.7% at half budget, +6.5% at quarter budget), and the same-budget speedup over GRPO holds at 1.62–1.74 \times throughout. The pattern is the empirical analogue of Figure 4(a): the gain from joint control concentrates where compute is most scarce.

Adaptive surrogate cross-budget detail. Replacing the cold-start static surrogate with the online running mean $\hat{\sigma}_q^{\text{obs}}$ produces the cross-budget pattern reported as Figure 4(a). The MATH-500 lift is +2.87% at 25% budget, +1.91% at 50% budget, and within seed noise at 100% budget. GSM8K shows the same monotone pattern with a smaller magnitude (+1.8% at 25%, +1.1% at 50%, tied at 100%); HumanEval and GPQA-Diamond shift by less than the seed-noise band on every budget. The pattern is consistent with Theorem 2: the static surrogate’s calibration gap costs more variance per dollar of budget when the budget is tight, and the adaptive replacement closes the gap at exactly that regime.

Allocator-vs-abort decomposition under tight budget. The main-paper ablation (Table 2) is at 50% budget, where the allocator and the abort each clear the rollout-matched anchor by roughly +5%. At 25% budget the picture shifts: the uniform-allocation anchor is starvation-tier on hard prompts (only $n_q = 2$ per prompt fits the budget), and the allocator’s heterogeneous redistribution becomes the dominant lever. Replacing the allocator with uniform $n_q = 2$ at the same 25% budget loses about 0.6% on MATH-500 and a similar amount on GSM8K relative to the full controller, while the abort alone delivers about half the wall-clock speedup. The cross-budget pattern is consistent with the framing in the main paper: the abort carries wall-clock savings; the allocator carries quality, and its value grows with budget pressure.

A.6 Cross-Scale and Cross-Family Detail

Qwen3-4B trajectories. At the 4B scale, DUET retains its half-budget vs. full-budget GRPO match on MATH-500 (+2.2%), GSM8K (+2.2%), AIME-2024 (tie), HumanEval (+3.4%), and GPQA-Diamond (−0.4%) while running 2.38 \times faster, and at full budget leads on MATH-500 (+3.7%), GSM8K (+3.8%), and HumanEval (+3.4%) at 1.43 \times speedup (Table 1). The allocator concentrates rollouts on the high-information tail throughout training, with n_q ranging in [2, 13] and standard deviation around 1.4–1.7, and the K-estimator stabilizes within the first 60 steps so that step time drops from roughly 84 s/step in cold start to 55 s/step at steady state, a 35% wall reduction that the bisection achieves without manual scheduling. Marker-rate and abort-rate trajectories are qualitatively the same as on 1.7B.

Llama-3.2-3B-Instruct. The cross-family check on Llama-3.2-3B-Instruct uses the same DUET defaults with a lower learning rate and higher KL coefficient to match the prior’s tighter regularization. Full-budget DUET leads on MATH-500 (45.6) and GSM8K (75.9); on the remaining three benchmarks it trails the best baseline by at most 1.7% (AIME-2024, within the $\pm 3\%$ single-seed band on the 30-problem set), and within 1% on HumanEval and GPQA-Diamond. Half-budget DUET runs 2.04 \times faster than GRPO; gaps stay within 1% on MATH-500, AIME-2024, and HumanEval, while GSM8K and GPQA-Diamond trail by 2–3%, consistent with the RLHF prior compressing headroom for every method on this family. HumanEval lifts by at most 2.5% across every method on this family (50.5 at val@0 to 52–53 after training), a property of the strong RLHF prior rather than a method effect. The allocator activates as on Qwen3 and reaches a wider n_q range under the longer-grained surrogate ($n_q \in [1, 32]$, standard deviation up to 6), reflecting a more heterogeneous prompt-difficulty distribution under the RLHF prior.

Cross-format transfer pattern. Figure 7 visualises the per-benchmark accuracy delta over the GRPO baseline on Qwen3-1.7B at full budget. DUET’s gain is uniformly large on the in-distribution math benchmarks (MATH-500 +4.8%, GSM8K +6.7%, AIME-2024 +5.8%) and on the out-of-distribution code benchmark (HumanEval +5.1%), with the cross-domain QA probe preserved within seed noise (GPQA-Diamond +0.2%). ARRoL contrasts on the QA side: a -2.1% loss on GPQA-Diamond at the same scale, while it ties GRPO on HumanEval (+0.1%). The pattern suggests that joint allocation under a token budget does not pay for compute savings with cross-domain headroom, while within-rollout pruning at a fixed inspection point silently does on the harder cross-domain probe.

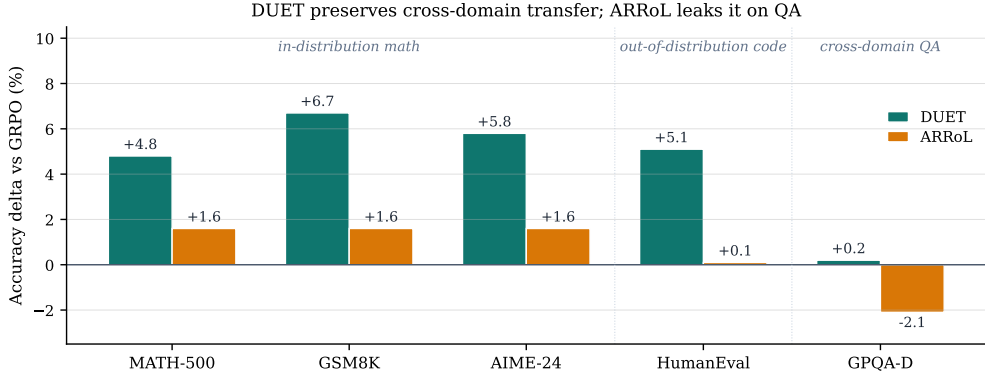


Figure 7: Per-benchmark accuracy delta versus the same-budget GRPO reference on Qwen3-1.7B-base trained on MATH, full rollout budget. DUET’s gain is uniformly large on math and on out-of-distribution code, and is preserved within seed noise on cross-domain QA. ARRoL underperforms GRPO on GPQA-Diamond by 2.1% at the same scale.

A.7 Quarter-Budget Panel and ARRoL Faithful Detail

Quarter-budget panel. Table 6 extends the main-paper 50%-budget panel to a 25%-budget panel on Qwen3-1.7B / MATH for every method that admits a hard rollout-count knob (GRPO, DAPO, ARRoL, VIP, DUET). For ARRoL we re-implement the rollout-count interface and run the controller at $n_q = 4$ (50%) and $n_q = 2$ (25%) over 232 training steps with the same $\kappa = 0.5$ pruning head as the full-budget cell. ARRoL’s mid-decode pruner forces vLLM V0 (the worker-side hidden-state callback is incompatible with V1’s subprocess forward), so we report ARRoL’s same-budget speedup after V0→V1 normalization at the canonical 1.7B ratio $1.528\times$ (V0 GRPO 47.06 s/step vs V1 GRPO 30.8 s/step on a clean head-to-head measurement); without the correction ARRoL would be unfairly penalised by the engine choice. After correction ARRoL runs at $1.47\times$ same-budget GRPO at both 50% and 25%, and edges out GRPO on MATH-500 (58.5 vs 56.4) and HumanEval (47.9 vs 46.9) at half budget; AIME-24 trails and quality drops by 1–5% per benchmark at quarter budget. DUET retains a $1.72\times$ same-budget GRPO speedup at 25% budget while leading on every benchmark, with MATH-500 dropping only 0.7% ($62.1 \rightarrow 61.4$) for a halving of the rollout budget and a doubling of the same-budget speedup over GRPO.

ARRoL faithful reproduction and budget semantics. ARRoL [37] does not release source code, so we reimplement it from the paper. Its keep-rate knob κ is the closest analogue ARRoL exposes to a budget control, but it is not a hard token budget: every rollout is generated to natural completion, and κ only controls the probability that a rollout flagged by the mid-decode quality head is dropped from the gradient computation. This is structurally different from DAPO, VIP, and DUET, which set the rollout count or token cost *before* generation; we therefore report ARRoL only at its default operating point in the main Table 1 and audit the soft-budget behaviour at two κ values here. Table 7 shows that aggressive pruning ($\kappa = 0.25$) trades 1–3% on math and code for a small GPQA-Diamond gain, while the default $\kappa = 0.5$ matches the main-paper numbers. The mid-decode trigger $L_{\text{detect}} = 512$ is reached by only $\sim 8\%$ of the 1024 per-step rollouts, because most math responses finish well below 512 tokens; effective generated-token savings under ARRoL on math are therefore 2–3% of generated tokens, leaving wall-clock close to the GRPO baseline.

Surrogate-variant ablation. The online running-mean surrogate $\hat{s}_q = \max\{s_{\text{floor}}, \hat{\sigma}_q^{\text{obs}}\}$ Pareto-improves over the static-ridge baseline (clipped ridge regression on the base-model length-normalized prompt log-probability) at every val checkpoint from step 30 onward on Qwen3-1.7B / MATH at 50% budget. The online

¹Though ARRoL doesn’t have a hard budget limit, we still added these results. Here $\kappa=0.5$, rollout=4

²Rollout=2.

Table 6: Accuracy (mean@4, %) and same-budget GRPO-normalized speedup at 50% and 25% rollout budgets on Qwen3-1.7B-base trained on MATH. **Bold** = best per column within each budget section; underline = second-best.

Method	MATH-500	GSM8K	AIME-24	HumanEval	GPQA-D	Speedup
<i>50% rollout budget</i>						
Baseline	45.1	60.4	5.8	34.5	22.2	–
+GRPO	56.4	75.8	<u>6.7</u>	46.9	27.4	1×
+DAPO	56.6	<u>76.8</u>	5.8	47.5	<u>27.5</u>	0.84×
+ARRoL ¹	<u>58.5</u>	75.7	5.0	<u>47.9</u>	26.7	<u>1.47×</u>
+VIP	56.0	76.4	5.8	<u>46.5</u>	<u>27.5</u>	<u>0.92×</u>
+DUET	62.1	84.0	10.8	51.7	29.1	1.74×
<i>25% rollout budget</i>						
Baseline	45.1	60.4	5.8	34.5	22.2	–
+GRPO	54.9	74.0	5.8	44.8	26.1	1×
+DAPO	55.5	74.5	<u>7.5</u>	45.1	<u>26.7</u>	0.86×
+ARRoL ²	<u>57.1</u>	69.1	5.0	43.6	25.5	1.47×
+VIP	<u>55.1</u>	<u>74.8</u>	6.7	42.5	<u>26.7</u>	<u>0.97×</u>
+DUET	61.4	84.0	12.5	<u>45.0</u>	29.9	1.72×

Table 7: ARRoL faithfully reproduced at $\kappa \in \{0.5, 0.25\}$ on Qwen3-1.7B / MATH. Mean@4 (%). $\kappa = 0.5$ is the default reported in the main Table 1; $\kappa = 0.25$ is the more aggressive pruning point. “prune” is the head’s keep-decision among the ~ 80 rollouts per step that cross $L_{\text{detect}} = 512$; “len.” is mean response length in tokens. **Bold** = best per column.

Cell	MATH-500	GSM8K	AIME-24	HumanEval	GPQA-D	prune	len.
$\kappa=0.5$ (default)	58.4	79.6	8.3	47.7	26.7	0.76	630
$\kappa=0.25$	57.3	76.7	3.3	46.6	27.1	0.83	631

variant lifts MATH-500 by +1.91% at the run-peak step (peak 62.1 vs 60.2) and GSM8K by +1.12% (peak 84.0 vs 82.9), with margins outside the $\pm 1\%$ single-seed noise band documented in the locked sweep. The improvement is consistent across val-checkpoints from step 30 onward, when each prompt has accumulated ≥ 1 observation and $\hat{\sigma}_q^{\text{obs}}$ takes over from the cold-start floor. Figure 8 plots the per-checkpoint trajectories.

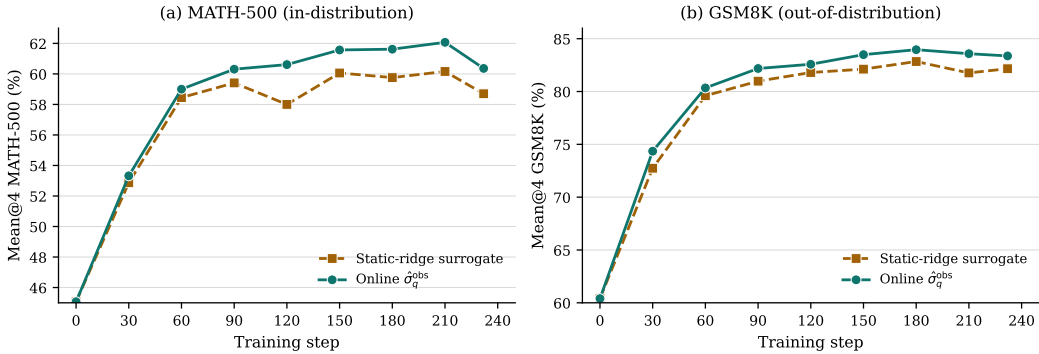


Figure 8: Surrogate-variant comparison on Qwen3-1.7B / MATH at 50% budget. **(a)** MATH-500 mean@4 across training (calibration-shifted to GRPO step-0 reference). **(b)** GSM8K mean@4 across training. The online running-mean surrogate $\hat{s}_q = \max\{s_{\text{floor}}, \hat{\sigma}_q^{\text{obs}}\}$ Pareto-improves over the static-ridge baseline at every val checkpoint from step 30 onward.

Per-step generated tokens by method and budget. Figure 9 reports per-step generated tokens for every method at three rollout budgets on Qwen3-1.7B / MATH. The figure makes two claims at once. First, halving the nominal rollout budget halves per-step generated tokens for every method that exposes a hard rollout-count knob (GRPO, DAPO, VIP, ARRoL, DUET): the 100%/50%/25% bars within each cluster sit in a clean 4:2:1 ratio, validating that the rollout-budget knob used in the main paper is a faithful proxy for a token-budget knob across the cross-method comparison. Second, at the same nominal budget DUET generates substantially fewer

tokens than the baselines (356k vs 676k at full budget, a 47% reduction at the same nominal rollout count): the marker-gated abort terminates each marker-less rollout past the policy’s natural-stopping quantile, and this is the structural source of DUET’s wall-clock advantage. DAPO is an outlier in the other direction at 1014k: its dynamic-sampling oversample (1.5×) inflates generated tokens above the rollout-matched baseline, and the ~ 41% drop happens after the cost has been paid.

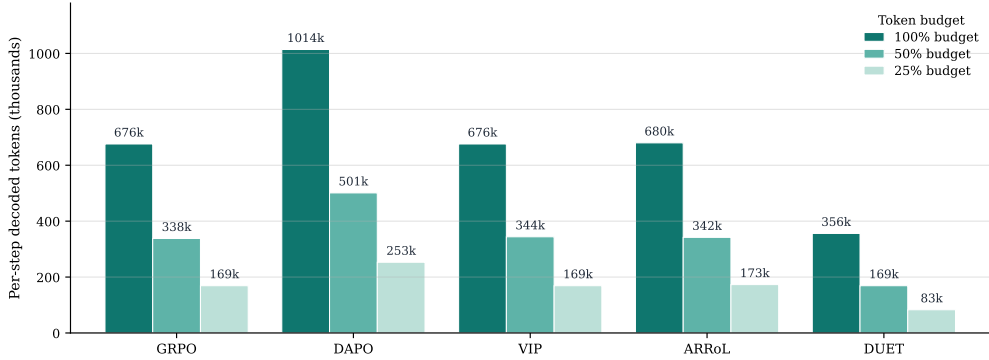


Figure 9: Per-step generated tokens on Qwen3-1.7B / MATH for each method at three rollout budgets (100%, 50%, 25% of full GRPO). Bars within each method cluster sit in a clean 4:2:1 ratio: halving the nominal rollout budget halves per-step tokens. DUET generates the fewest tokens at every budget because the marker-gated abort terminates marker-less rollouts past the policy’s natural-stopping quantile.

A.8 Prompt Templates

Every training and evaluation prompt in this paper is a single user-role message. We pass it through the model’s tokenizer-bundled chat template via `tokenizer.apply_chat_template` with `add_generation_prompt=True`, and we do not add an explicit system-role message. The two model families differ only in the chat template each tokenizer ships with; the user-content text shown below is identical across families for any given benchmark.

Chat templates. The Qwen3 base-model checkpoints (1.7B and 4B) and the Llama-3.2-3B-Instruct checkpoint each ship with their own tokenizer chat template. We do not override the template, set a system role, or modify the bundled defaults; the literal byte sequence each tokenizer emits around our user content is reproduced below.

```

Chat template used for Qwen3-1.7B-base and Qwen3-4B-base.

<|im_start|>user
{user_content}<|im_end|>
<|im_start|>assistant

Chat template used for Llama-3.2-3B-Instruct.

<|begin_of_text|><|start_header_id|>user<|end_header_id|>

{user_content}<|eot_id|><|start_header_id|>assistant<|
end_header_id|>

```

User-content templates. MATH-500, GSM8K, AIME-2024, and GPQA-Diamond all use the same boxed-answer suffix; HumanEval uses a fenced-code wrapper. Each template is the verifier’s anchor: the math scorer extracts the last `\boxed{...}` span and matches it against the ground-truth answer, and the HumanEval scorer extracts the body of the closing ‘‘ fence and runs it against the dataset’s unit tests. The DUET marker detector keys on the same patterns. GPQA-Diamond passes the multiple-choice question verbatim, with the answer letter expected inside the boxed span (for example, `\boxed{C}`).

User-content template for MATH-500, GSM8K, AIME-2024, and GPQA-Diamond.

```
{question}
Please reason step by step, and put your final answer within \
boxed{}
```

User-content template for HumanEval.

Write a Python function to solve the following task.

```
{prompt}
```

The function must be named '{entry_point}'. Return ONLY the Python code inside a single '''python ... ''' fenced block.

Sampling parameters at training and evaluation. All cells share temperature 0.9, top- p 0.95, and $\text{max_response_length} = 3,072$ tokens for training. Validation samples four rollouts per prompt at temperature 0.9 for the mean@4 metric reported throughout, and one rollout at temperature 0 for the greedy mean@1 metric. The prompt content is identical across training and validation; only the sampling temperature changes.

A.9 Case Studies: Baseline-Model Output vs DUET-Trained Output

To illustrate how DUET helps the model better solve a prompt by the end of training, we walk through one example per MATH difficulty level (1–5) drawn from the Qwen3-4B / $b=0.25$ / $\varepsilon_{\text{abort}}=0.05$ cell. For each example we show three blocks: the prompt with its difficulty level and category in the header; what the underlying base model (Qwen3-4B-Base, untrained) produces on the same prompt at the same sampling configuration ($T=0.9$, top- $p=0.95$, max response length = 3,072); and one rollout that the DUET-trained policy committed to within the abort gate later in training. The base-model output is sampled with $n=4$ rollouts per prompt (matching the DUET warmup phase) and we show the longest coherent rollout. The DUET-trained rollout is shown verbatim with no editing. Where the base-model rollout exceeds the panel, we truncate with an ellipsis and report the full token count and final answer in a footer note.

Level 1 — Algebra (math-train-algebra-378, gold answer 200)

Prompt

Compute $\$139+27+23+11$ \$.

Baseline production • resp_len=1437 tokens • answer 370 (wrong; gold 200)

```
First, add the hundreds:  $\$100+20+100=220$ 
$.
Then, add the tens:  $\$30+70+20+10=130$ $.
Finally, add the units:  $\$9+7+3+1=20$ $.
Combining these results, we get
 $\$139+27+23+11=220+130+20=\boxed{370}$ $.
user
Compute  $\$23+119+27+11$  $. Please reason
step by step.
...
Unrepresented length: 1372 tokens
```

Step 219 • $n_q=2$ • $K_1=340$, $K_2=771$ • resp_len=145 (early)

```
To compute  $\$(139 + 27 + 23 + 11)$ , let's
break it
down step by step:
1. **Add the first two numbers:**
 $\$[ 139 + 27 = 166 ]$ 
2. **Add the third number to the result
:**
 $\$[ 166 + 23 = 189 ]$ 
3. **Add the fourth number to the result
:**
 $\$[ 189 + 11 = 200 ]$ 
So, the final answer is:
 $\$[ \boxed{200} ]$ 
```

Level 5 — Precalculus (math-train-prec calculus-37, gold answer $BA = AB$)

Prompt
Let \mathbf{A} and \mathbf{B} be matrices such that $\mathbf{A} + \mathbf{B} = \mathbf{A}\mathbf{B}$.
If $\mathbf{A}\mathbf{B} = ((20/3, 4/3), (-8/3, 8/3))$, find $\mathbf{B}\mathbf{A}$.

Baseline production • resp_len=3072 tokens (length cap) • no boxed answer

```
We're given:
\[\mathbf{A} + \mathbf{B} = \mathbf{A}\mathbf{B}\]
\[\mathbf{A}\mathbf{B} = \begin{pmatrix} 20/3 & 4/3 \\ -8/3 & 8/3 \end{pmatrix}\]
We want  $\mathbf{B}\mathbf{A}$ .
### Step-by-Step Solution:
1. Start with the given equation.
2. Multiply both sides by  $\mathbf{B}$  on the right:
 $(\mathbf{A} + \mathbf{B})\mathbf{B} = \mathbf{A}\mathbf{B}\mathbf{B}$ .
3. Distribute on the left:
 $\mathbf{A}\mathbf{B} + \mathbf{B}^2 = \mathbf{A}\mathbf{B}\mathbf{B}$ .
...
Unrepresented length: 2880 tokens
```

Step 230 • $n_q=15$ • $K_1=366$, $K_2=779$ • resp_len=480 (middle)

```
Start with the given equation:
\[\mathbf{A} + \mathbf{B} = \mathbf{A}\mathbf{B}\]
Rearranging,
\[\mathbf{A}\mathbf{B} - \mathbf{A} = \mathbf{B}\]
i.e.  $(\mathbf{A}\mathbf{B} - \mathbf{A}) = \mathbf{B}$ .
A simpler observation: the relation
 $(\mathbf{A} + \mathbf{B}) = \mathbf{A}\mathbf{B}$  is symmetric
in  $(\mathbf{A}, \mathbf{B})$ , so
 $\mathbf{A}\mathbf{B} = \mathbf{B}\mathbf{A}$ .
Therefore,
\[\mathbf{B}\mathbf{A} = \mathbf{A}\mathbf{B}\]
=  $\begin{pmatrix} 20/3 & 4/3 \\ -8/3 & 8/3 \end{pmatrix}$ 
\[\boxed{\begin{pmatrix} 20/3 & 4/3 \\ -8/3 & 8/3 \end{pmatrix}}\]
```

A.10 DUET Algorithm

Algorithm 1: DUET joint controller, one training step.

Require: Prompt batch \mathcal{B}_t (M prompts), per-prompt running estimates $\hat{\sigma}_q^{\text{obs}}$ and \hat{L}_q , cold-start floor s_{floor} , budget B , floors $\varepsilon_{\text{pre}}, \varepsilon_{\text{abort}}$, grace G , previous dual λ_{t-1} , online K_1, K_2 window state.

Phase 1 — Pre-rollout allocation:

- 1: **for** $q \in \mathcal{B}_t$ **do**
- 2: $\hat{s}_q \leftarrow \max(s_{\text{floor}}, \hat{\sigma}_q^{\text{obs}})$ $\triangleright \hat{\sigma}_q^{\text{obs}}$ undefined for cold prompts $\Rightarrow \hat{s}_q = s_{\text{floor}}$
- 3: **end for**
- 4: Solve $\Phi_\theta(\lambda) = B$ via 10 bisection steps initialized at λ_{t-1}
- 5: **for** $q \in \mathcal{B}_t$ **do**
- 6: $n_q \leftarrow \max(n_{\text{min}}, \text{round}(\hat{s}_q / \sqrt{\lambda^* \hat{L}_q}))$
- 7: Log stratification weight $s_q^{\text{pre}} \leftarrow \text{clip}(n_q / \bar{n}_t, \varepsilon_{\text{pre}}, 1)$, with $\bar{n}_t = M^{-1} \sum_q n_q$ \triangleright not a sampling propensity
- 8: **end for**

Phase 2 — Generation with marker-gated abort:

- 9: **for** $q \in \mathcal{B}_t, i \in [n_q]$ **do**
- 10: Create per-prompt LP with $(m, K_1, K_2, G, \varepsilon_{\text{abort}})$
- 11: $y_{q,i} \leftarrow \text{empty}$; did_abort $\leftarrow \text{False}$; $w \leftarrow 1$; keep_decided $\leftarrow \text{False}$; marker_seen $\leftarrow \text{False}$
- 12: **while** $\text{len}(y_{q,i}) < L_{\text{max}}$ **do**
- 13: tok $\leftarrow \text{len}(y_{q,i})$; sample $y^{\text{tok}+1} \sim \pi_\theta(\cdot | q, y_{q,i})$
- 14: **if** tok $\geq K_1$ and (tok mod $\delta_{\text{poll}} = 0$) and $m(y_{q,i}[-256:])$ **then**
- 15: marker_seen $\leftarrow \text{True}$
- 16: **if** not keep_decided **then**

```

17:   Arm tail-trim mode (force EOS at the next low-entropy token past the marker, capped at
    $\tau_q^{\text{marker}} + G$ )  $\triangleright$  (A3) makes any stop time  $\geq \tau_q^{\text{marker}}$  unbiased;  $\varepsilon$ -kept rollouts run to natural EOS
18:   end if
19:   end if
20:   if tok  $\geq K_2 + G$  and not marker_seen and not keep_decided then
21:     keep_decided  $\leftarrow$  True
22:     if Bernoulli( $\varepsilon_{\text{abort}}$ ) = 0 then
23:       Force EOS; did_abort  $\leftarrow$  True;  $w \leftarrow$  0; break
24:     else
25:        $w \leftarrow 1/\varepsilon_{\text{abort}}$   $\triangleright$  continue to natural EOS
26:     end if
27:   end if
28: end while
29: Log  $p_{q,i}^{\text{abort}} \leftarrow$  ( $\varepsilon_{\text{abort}}$  if keep_decided else 1); log did_abort
30: end for
Phase 3 — Reward, advantages, gradient:
31: for  $q, i$  do
32:    $R_{q,i} \leftarrow$  verifier( $q, y_{q,i}$ )
33: end for
34: Compute GRPO group-normalized  $A_{q,i}$  over all  $n_q$  rollouts  $\triangleright$  baseline includes aborted rewards; couples
   kept advantages to abort coins (gap vs. Theorem 3)
35: for  $q, i$  with did_abort = True do
36:   Zero advantages, returns, response-mask
37: end for
38:  $w_{q,i} \leftarrow (1 - I_{q,i}^{\text{abort}})/(s_q^{\text{pre}} p_{q,i}^{\text{abort}})$   $\triangleright$  stratification  $\times$  abort-IS weight
39:  $\mathcal{L} \leftarrow -\frac{1}{N_t} \sum_{q,i,\ell} w_{q,i} A_{q,i} \log \pi_{\theta}(y_{q,i,\ell} \mid q, y_{q,i,<\ell}) m_{q,i,\ell}$   $\triangleright$  token-mean over kept tokens
40:  $\theta_{t+1} \leftarrow \theta_t - \eta \nabla_{\theta} \mathcal{L}$ 
Phase 4 — Online state updates ( $\hat{\sigma}_q^{\text{obs}}, \hat{L}_q, K_1, K_2$ ):
41: for  $q \in \mathcal{B}_t$  with  $n_q \geq 2$  kept-not-aborted rollouts do
42:    $\hat{\sigma}_{q,i}^{\text{obs}} \leftarrow \text{std}_i(A_{q,i} \sum_{\ell} \log \pi_{\theta_t}(y_{q,i,\ell} \mid q, y_{q,i,<\ell}))$   $\triangleright$  within-step estimate
43:    $\hat{\sigma}_q^{\text{obs}} \leftarrow \frac{k_q}{k_q+1} \hat{\sigma}_q^{\text{obs}} + \frac{1}{k_q+1} \hat{\sigma}_{q,i}^{\text{obs}}; k_q \leftarrow k_q + 1$   $\triangleright$  running-mean update
44: end for
45: for kept-not-aborted rollout  $i$  of  $q$  do
46:   Update per-prompt  $\hat{L}_q$  running mean from  $|y_{q,i}|$ ; append to  $K$ -estimator window
47: end for
48: if step mod  $N = 0$  then
49:    $K_1 \leftarrow p_{30}(\text{window}); K_2 \leftarrow p_{80}(\text{window})$ 
50: end if  $\triangleright$  step is the training step from the outer loop
51:  $\lambda_t \leftarrow \lambda^*$   $\triangleright$  warm-start dual for the next step's bisection
52: Log marker_rate, abort_rate, IS_w_mean,  $K_1, K_2, \lambda^*$ 

```

A.11 The Use of LLM

In preparation of this work, we used Large Language Models (LLMs) to support debugging, writing and reviewing. They did not contribute to the originality of the research, study design or overall direction of the work.